JCTC Journal of Chemical Theory and Computation

Article

Cite This: J. Chem. Theory Comput. 2017, 13, 6237−6252

pubs.acs.org/JCTC

Accurate Excited-State Geometries: A CASPT2 and Coupled-Cluster Reference Database for Small Molecules

Šimon Budzák,[†] Giovanni Scalmani,[‡] and Denis Jacquemin*[,§,∥]

[†]Department of Chemistry, Faculty of Natural Sciences, Matej Bel University, Tajovského 40, SK-97400 Banská Bystrica, Slovak Republic

[‡]Gaussian Incorporated, 340 Quinnipiac Street, Building 40, Wallingford, Connecticut 06492 United States

[§]Laboratoire CEISAM−UMR CNRS 6230, Université de Nantes, 2 Rue de la Houssinière, BP 92208, 44322 Cedex 3 Nantes, France

[∥]Institut Universitaire de France, 1 Rue Descartes, 75231 Cedex 5 Paris, France

Supporting Information

ABSTRACT: We present an investigation of the excited-state structural parameters determined for a large set of small compounds with the dual goals of defining reference values for further works and assessing the quality of the geometries obtained with relatively cheap computational approaches. In the first stage, we compare the excited-state geometries obtained with ADC(2), CC2, CCSD, CCSDR(3), CC3, and CASPT2 and large atomic basis sets. It is found that CASPT2 and CC3 results are generally in very good agreement with one another (typical differences of ca. 3×10^{-3} Å) when all electrons are correlated and when the aug-cc-pVTZ atomic basis set is employed with both methods. In a second stage, a statistical analysis reveals that, on the one hand, the excited-state (ES) bond lengths are much more sensitive to the selected level of theory than their ground-state (GS) counterparts and, on the other hand, that CCSDR(3) is probably the most cost-effective method delivering accurate structures. Indeed, CCSD tends to provide too compact multiple bond lengths on an almost systematic basis, whereas both CC2 and ADC(2) tend to exaggerate these bond distances, with more erratic error patterns, especially for the latter method. The deviations are particularly marked for the polarized CO and CN bonds, as well as for the puckering angle in formaldehyde homologues. In the last part of this contribution, we provide a series of CCSDR(3) GS and ES geometries of medium-sized molecules to be used as references in further investigations.

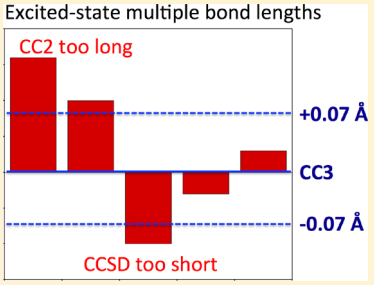

1. INTRODUCTION

During the past decade, the focus of the theoretical works investigating electronically excited states (ESs) has moved from the determination of vertical transition properties obtained on a frozen ground-state (GS) geometry to the exploration of the potential energy surfaces (PES) of these ESs.[1] Indeed, characterizing regions away from the Franck−Condon point is of crucial importance for many key applications, e.g., photochromism, long-range electron transfer, and fluorescence.[2] In turn, this interest has motivated the development of analytical gradients for numerous ES methods,[3−14] paving the way to computationally efficient calculations of the ES PES. Nevertheless, a balanced assessment of the accuracy of these gradients, and, as a consequence of the optimal ES geometries (and possibly conical intersections, CIs) obtained through theory, is far from straightforward. Indeed, experimental ES geometries are available for a small number of compact (typically two to six atoms) fluorescent derivatives only, contrasting with the plethora of available GS structures, that can now be accurately determined with advanced approaches combining theory and experiment.[15] More importantly, the experimental determinations of ES structures often imply quite large error bars and the values of some parameters have to be assumed or frozen during the fitting procedures. Therefore, assessing the accuracy of a particular theory using experimental ES structures is de facto not a very satisfying approach. As an alternative, one can use indirect experimental signatures of the PES to evaluate the pros and cons of a given level theory. More specifically, the topologies of the absorption and emission bands resulting from strong vibronic couplings have been used to estimate the qualities of ES PES given by theory.[2,16−19] Such an approach is interesting because large molecules can be considered, but one is limited, on the one hand, to compounds displaying well-defined band shapes, that is, quite rigid dyes, and, on the other hand, by the use of the harmonic approximation that significantly affects the computed vibrational frequencies, making it difficult to determine if the discrepancies between the measured and calculated spectra are related to this approximation[20] or to the intrinsic limitations of the selected electronic structure theory. Therefore, purely theoretical benchmarks of ES geometries, in which a higher level of theory is used as reference to gauge the performances of a lower level of theory, remain of interest. Unsurprisingly, several studies of this kind have appeared,[21−25] but these works are typically limited, on the one hand, by the quality of the

Received: August 31, 2017
Published: November 15, 2017

DOI: 10.1021/acs.jctc.7b00921
J. Chem. Theory Comput. 2017, 13, 6237−6252

reference data used and, on the other hand, by the lack of Hessian calculations making it impossible to ascertain the nature (minimum, transition state, and so on) of the final structures. We briefly describe the most advanced sets of ES structures available to date for generic molecules. First, in 2003, Page and Olivucci obtained complete active space with second-order perturbation theory (CASPT2) geometries for a series of ESs of $n \rightarrow \pi^*$ (acrolein, acetone, diazomethane, and propanoic acid anion), $\pi \rightarrow \pi^*$ (*trans*-/*cis*-butadiene and pyrrole) and cyanine (two model protonated Schiff bases containing five and nine atoms in the conjugated path) natures.[26] This work certainly represented a huge computational effort at that time, but symmetry constraints were imposed in some cases (e.g., C_{2v} for the lowest ES of acetone) and the compact 6-31G(d) atomic basis set was used for most compounds. Ten years later, symmetry-adapted cluster−configuration interaction (SAC−CI) structures have been obtained with a polarized double-ζ atomic basis set, namely, D95(d,p), by Bousquet and co-workers for both the singlet[23] and triplet[24] ES of medium-sized compounds: furan, pyrrole, pyridine, *p*-benzoquinone, uracil, adenine, coumarin, 9,10-anthraquinone, and 1,8-naphthalimide. Again, symmetry constraints were imposed in both these works to avoid conical intersections, though frequency calculations (CIS level) were carried out to ascertain the nature of the optimized states. In 2012, Jagau and Gauss obtained Mukherjee's multireference coupled-cluster singles and doubles (Mk-MRCCSD) GS and ES geometries (cc-pCVTZ basis set) of eight closed-shell molecules (acetylene, cyclopentadiene, furan, naphthalene, pyrrole, tetrazine, thiophene, and vinylidene) and several radicals.[27] In 2013, Guareschi and Filippi proposed what probably stands as the most accurate theoretical set of reference ES structures available to date by determining quantum Monte Carlo (QMC) ES geometries with the pVTZ′ atomic basis set for five small molecules (acetone, *trans*- and *cis*-acrolein, methylenecyclopropene, and the propanoic acid anion).[28] The QMC variant used in ref 28, namely, variational Monte Carlo (VMC), was shown to provide mean absolute errors (MAEs) of ca. 0.004 Å for diatomics, using experimental values as references.[29] In the field of geometrical ES benchmarks, one should also mention the contributions of Olivucci and co-workers who performed several investigations dedicated to the exploration of the ES PES of retinal derivatives.[30−33] As can be concluded from this literature survey, the number of highly accurate reference ES geometries available to date remains rather small, and the present work constitutes a further effort in that direction.

Today, most ES geometry optimizations are performed with the complete active space self-consistent field (CASSCF) or with the time-dependent density functional theory (TD-DFT)[34] approaches. The former is able to describe CIs and hence to model photochemical events but lacks dynamical correlation and cannot, therefore, be viewed as an accurate reference approach for obtaining ES geometries. The latter, a single-reference approach, is particularly popular because it can deliver very satisfying results, but this requires one to choose an exchange−correlation functional (XCF) "adequate" for the studied case: a choice which is far from trivial.[35] The interested reader can indeed find several TD-DFT benchmarks devoted to ES structures, for both small- and medium-sized compounds,[5,9,21−25,28,36] but again the quality of the selected reference probably remains an open question. Alternatively, one can turn toward the simplest linear-response coupled-cluster approach, namely CC2,[37−39] or the second-order algebraic diagrammatic construction method [ADC(2)][40] that both allow tackling quite large compounds (ca. 30−50 atoms) and do not involve the choice of an XCF. However, these methods were reported to overestimate some bond lengths especially for the keto group,[6,22,25,28,41] and caution is necessary before using them as references.

Compared to previously reported works, the present contribution has several specificities. First, we have decided to systematically compute ES Hessian at a reasonable level of theory, so to ascertain the nature of the obtained geometries. To this end, we have selected the (EOM-)CCSD level. Second, we have used a strategy relying on, on the one hand, the CC hierarchy, that is CC2,[37−39] CCSD,[42−45] CCSDR(3),[46] and CC3,[37,47] and, on the other hand, the CASPT2 method,[48,49] to be able to assess the consistency of the results generated by these approaches, as well as, to estimate the importance of multireference effects. We note that more advanced methods such as as XMCQDPT2,[50] which accounts for state mixing in a more accurate way, or QMC could also be used but, to date, they remain less widely available than CASPT2. Third, we selected reasonably large atomic basis sets, that is, def2-TZVPP, ANO-L-VQZP, and aug-cc-pVTZ, to obtain accurate results, a claim that cannot be made when using double-ζ bases for highly correlated methods. Indeed, these three basis sets include, at least, d and f orbitals for hydrogen atoms and second-/third-row atoms, respectively. Fourth, we have considered compounds with more diverse nuclei than in previous works, including sulfur, selenium, fluorine, chlorine, and bromine atoms, in order to expand the scope of the conclusions. Therefore, beyond providing a set of reference data, we are also able here to assess the relative accuracies of ADC(2), CC2, and CCSD ES geometries.

2. COMPUTATIONAL DETAILS

The EOM-CCSD calculations have been performed with the Gaussian development and Gaussian-16 codes[51] and consisted of geometry optimizations of GS and ES performed with both def2-TZVPP and aug-cc-pVTZ atomic basis sets, and subsequent vibrational frequency determinations with the former basis. The energy and geometry convergence thresholds were systematically tightened, with requested convergence of 10^{-10}− 10^{-11} au for the SCF energy and a residual mean smaller than 10^{-5} au for the forces. During the CC calculations, all electrons including the core ones were correlated (so-called *full* option) and the CCSD energy convergence threshold was set to 10^{-8}−10^{-9} au, whereas the EOM-CCSD energy convergence was tightened to 10^{-7}−10^{-8} au, to obtain accurate analytical gradients allowing for stable numerical differentiations leading to the Hessian.[52] The T_1 diagnostic test of multiconfigurational character[53] was computed for all compounds at the CCSD/def2-TZVPP level, and values are given in the Supporting Information (SI). We recall that $T_1 > 0.02$ indicates that a multireference method is needed to obtain an accurate description.[53] As can be seen in the SI, the computed T_1 values are almost always systematically smaller than this threshold. The ADC(2) and CC2 optimizations have been performed with the Turbomole package,[54] selecting the same atomic basis sets as in the EOM-CCSD calculations and applying the resolution-of-identity approximation. During these calculations, the SCF, second-order and geometry optimization thresholds were all set to stricter-than-default values, that is, 10^{-9}, 10^{-7}, and 10^{-5} au, respectively, whereas we also correlated all electrons to obtain results comparable to the one of the

DOI: 10.1021/acs.jctc.7b00921
J. Chem. Theory Comput. 2017, 13, 6237−6252

Table 1. Geometrical Parameters (Bond Lengths, Å; Valence Angles, Degrees) for the Lowest A_u and A_2 ES of acetylene in the C_{2h} and C_{2v} Point Groups, Respectively[a]

	A_u excited state			A_2 excited state			
method	C≡C	C−H	C≡C−H	C≡C	C−H	C≡C−H	ref
ADC(2)/aug-cc-pVTZ	1.369	1.086	122.1	1.345	1.087	132.1	this work
CC2/aug-cc-pVTZ	1.377	1.086	122.0	1.349	1.088	132.2	
CCSD/aug-cc-pVTZ	1.352	1.086	124.1	1.322	1.088	135.4	
CCSDR(3)/aug-cc-pVTZ	1.368	1.090	122.3	1.340	1.093	132.4	
CC3/aug-cc-pVTZ	1.371	1.090	122.2	1.342	1.093	132.9	
CASPT2(10e,10o)/aug-cc-pVTZ	1.370	1.092	122.2	1.342	1.094	132.4	
MR-AQCC/extrapol.	1.369	1.091	123.2	1.339	1.093	132.9	65
Mk-MRCCSD/cc-pVCTZ	1.368	1.093	123.3	1.337	1.095	132.5	27
experiment	1.375	1.097	122.5				61

[a]See Table S1 in the SI for further data and details.

EOM-CCSD calculations. ADC(2) and CC2 numerical frequency calculations were also systematically performed with the def2-TZVPP atomic basis set. The CCSDR(3) and CC3 calculations were performed with the Dalton package[55] using the same two basis sets as those for the other CC models. These optimizations used default convergence thresholds, and all electrons were correlated. We underline that analytical gradients are not available for these two levels of theory, so that the CCSDR(3) and CC3 minimizations were based on numerical differentiation of the total energies, a task that is extremely computationally intensive for these two methods. For the records, we have compared CCSDR(3)/aug-cc-pVTZ and CCSDR(3)/cc-pVQZ ES geometries of both acetylene and formaldehyde and found rather small differences.[56] CASPT2 calculations were performed with the OpenMolcas 8.3 software,[57,58] and the active orbital energies were corrected by the usual 0.25 au IPEA shift. For transition energies, discussions about the impact of the IPEA shift can be found elsewhere,[59] and it was concluded that such IPEA improves the agreement with reference values when a large atomic basis set is used. Initially, we treated the compounds using the frozen-core model and the large atomic natural orbital (ANO-L) basis set with VQZP contraction scheme to obtain first estimations. Such an approach is typically applied in highly accurate CASPT2 calculations. Second, we have done the calculations with the aug-cc-pVTZ atomic basis set and no frozen orbitals to offer results directly comparable to their CC counterparts. To speed up the calculations, we applied Cholesky decomposition technique[60] with the 10^{-4} decomposition threshold. We compared formaldehyde GS/ES geometries obtained with and without Cholesky decomposition and found, as expected, no significant difference. We are aware of recent developments on analytical CASPT2 gradients,[13,14] but for practical reasons we used Molcas where the analytical gradients are not available, and we consequently relied on numerical gradients. The convergence thresholds were 10^{-12}, 10^{-6}, and 10^{-9} au for CASSCF energy, orbital rotation, and the norm of the CASPT2 residual, respectively. The geometry optimization was considered converged when the root mean square (rms) of gradients in internal coordinates was less than 10^{-6}. Unlike CC methods, CASPT2 cannot be used in a black-box fashion as the obtained results are sensitive to the choice of active space. The active space choices used for all molecules are rather large and are detailed in the SI. Usually the full valence active space was used and, in several cases, further extended by additional virtual orbitals. As a final comment, note that in the following, we use as the naming convention for bond nature (single or double) the GS Lewis structures, which is the natural choice in chemistry, though the bonding nature might change in the ES.

3. RESULTS AND DISCUSSION

A complete list of results, including Cartesian coordinates, GS and ES geometrical parameters and comparison with literature data, is available in the SI. We discuss only key results below, mainly focusing on the ones obtained with the basis set containing diffuse functions.

3.1. Acetylene. Acetylene is the most compact π-conjugated molecule for which the optimized geometries of low-lying $\pi \rightarrow \pi^*$ ESs do not correspond to a conical intersection. Nevertheless, the lowest ESs are known to break the cylindrical symmetry of the GS and both C_{2h} and C_{2v} minima can be obtained. To our knowledge, the only available experimental results concern the lowest A_u ES, for which the most recent measurements predict a CC bond length of 1.375 Å and a CCH valence angle of 122.5°,[61] in reasonable match with earlier experimental estimates.[62] In contrast, there is already a vast amount of theoretical data,[25,27,63−65] among which one finds a detailed MR-AQCC investigation[65] and a multireference CCSD work.[27] We have investigated three low-lying ES (A_u, B_u and A_2 symmetry), and we list some key ES structural data for the two lowest lying states in Table 1.

All methods agree that a substantial elongation of the carbon−carbon triple bond takes place after photon absorption and that this elongation is larger in the A_u ES than in the A_2 state. Nevertheless the absolute C≡C ES length significantly depends on the selected method. While the three most refined approaches, that is, CC3, CASPT2, and MR-AQCC, yield very consistent estimates (maximal discrepancy of 0.003 Å), one notices that CC2 provides significantly too long C≡C bonds whereas CCSD gives the opposite error. Interestingly, similar trends can be noticed for the GS structure, though, in that case, the differences between the various CC approaches are much less marked (see Table S1 in the SI). Eventually, we note that the perturbative CCSDR(3) method allows correcting the largest part of the CCSD error, and the CCSDR(3) estimates are not differing by more than 0.002 Å from the CC3 and MR-AQCC ones. For both the A_u and A_2 ES, the CASPT2 calculations deliver a strongly dominating single-reference character (0.94 weight at the GS geometry), so that we consider our CC3/aug-cc-pVTZ values as the most accurate. In contrast, the B_u ES can be described as a combination of two monoexcitations having 0.34 and 0.61 weights. Although CC

DOI: 10.1021/acs.jctc.7b00921
J. Chem. Theory Comput. 2017, 13, 6237−6252

Table 2. Geometrical Parameters (Bond Lengths, Å; Valence Angles and Dihedral Angle, Degrees) for the Lowest ES of Formaldehyde[a]

method	C=O	C−H	H−C−H	η	ref
ADC(2)/aug-cc-pVTZ	1.380	1.081	123.8	18.9	this work
CC2/aug-cc-pVTZ	1.353	1.085	121.3	29.5	
CCSD/aug-cc-pVTZ	1.300	1.087	118.9	30.9	
CCSDR(3)/aug-cc-pVTZ	1.320	1.089	118.2	36.6	
CC3/aug-cc-pVTZ	1.326	1.089	118.3	36.8	
CASPT2(12e,10o)/aug-cc-pVTZ	1.326	1.090	118.1	38.2	
MR-AQCC/extrapol.	1.325	1.090	117.4	34.9	71
CR-EOM-CCSD(T)/cc-pVTZ	1.325			32.5	66
experiment	1.323	1.098	118.4	34	69

[a] η is the puckering angle measuring how the C=O bond is out of the HCH plane. See Table S2 in the SI for complete data.

Table 3. Geometrical Parameters (Bond Lengths, Å; Valence Angles, Degrees) for the Lowest ES of Thioformaldehyde and Selenoformaldehyde[a]

	thioformaldehyde			selenoformaldehyde			
method	C=S	C−H	H−C−H	C=Se	C−H	H−C−H	refs
ADC(2)	1.725	1.079	121.0	1.863	1.078	121.3	this work
CC2	1.710	1.079	120.8	1.843	1.078	121.2	
CCSD	1.682	1.077	119.4	1.813	1.076	119.5	
CCSDR(3)	1.705	1.078	120.1	1.838	1.077	120.1	
CC3	1.709	1.078	120.2	1.843	1.077	120.3	
CASPT2(12e,15o)	1.711	1.079	120.3	1.845	1.077	120.3	
experiment	1.682	1.077	120.7	1.856		121.6	69, 74, and 78

[a] All theoretical results obtained with the aug-cc-pVTZ atomic basis set. See Tables S3 and S4 for additional data.

methods should be reliable in cases involving combination of monoexcitations, and although the CCSD T_1 diagnostic returns a 0.015 value for the B_u geometry, we note that the CC3 and CASPT2 difference are more marked, e.g., 0.007 Å for the C≡C bond length of that ES (see Table S1 in the SI) and we consider the CASPT2 values as more reliable for the B_u state.

3.2. Formaldehyde. Formaldehyde is one of the most investigated systems, and a plethora of experimental and theoretical publications can be found in the literature.[66] It is well-recognized that in the lowest n → π^* ES, the carbonyl bond significantly lengthens as the molecule departs from planarity. All available measurements fall in the quite narrow range of 1.323 ± 0.002 Å for the ES C=O distance,[67−69] and this value can therefore be used as a reference. In contrast, the experimentally reported estimates for the puckering angle cover a broader range of values: 20.5°,[67] 31.1°,[67] and 34.0°.[68−70] Interestingly, the two first data originate from the same work that analyzed both the 0° and 4^1 bands, illustrating the difficulty to obtain very reliable experimental results, even for a hallmark tetratomic compound. Table 2 summarizes the results that we obtained for formaldehyde and compares them to previous high-level reference calculations (see Table S2 in the SI for complete data). The highest levels of theory available, i.e., CC3, CASPT2, MR-AQCC,[71] and CCSD(T)[66] all provide very similar C=O bond length in very good agreement with the measurements. As expected from previous works (see Introduction), CC2 predicts a significantly too long carbonyl bond in the ES, whereas, probably less expected, though similar to the acetylene case, is the fact that the CCSD bond length is too short. ADC(2) also significantly overshoots the C=O bond length. Qualitatively, the same errors are found for the GS structure, but the quantitative extent of the discrepancies is smaller than in the ES. Consequently, the elongation of the carbonyl bond upon electronic transition, that reaches +0.119 ± 0.001 Å with the four most refined approaches, is overestimated by both ADC(2) (+0.171 Å) and CC2 (+0.137 Å) but underestimated (+0.100 Å) by CCSD. CCSDR(3) is probably a reasonable compromise, as it improves significantly the CCSD estimate (+0.113 Å) for a lower computational cost than CC3. For the C−H bond length, all methods but ADC(2) provide very similar values and this statement holds for both the GS and ES. The H−C−H angle is more sensitive to the level of theory, ADC(2), CC2 (to a large extent), and CCSD (to a smaller extent) overshooting the reference value (see also Table S2). In contrast the puckering angle, η, is too small with these three methods, with a large error for ADC(2). This parameter is obviously quite sensitive to the level of theory used. As the CASPT2 calculations did not reveal a significant multiconfigurational character (weight of leading determinant larger than 0.95), we consider the CC3/aug-cc-pVTZ value of 36.8° to be the most accurate estimate available to date. Eventually, an extra parameter of interest is the inversion barrier, that is, the relative energy of the transition state corresponding to a planar ES geometry. The experimental values reported for this barrier are 350 cm^{-1},[69] 356 cm^{-1},[72] 356 cm^{-1},[70] and 316 cm^{-1}.[68] This last value is probably the most realistic, as it is a *true potential* estimate; a 350 cm^{-1} barrier is obtained in ref 68. for the *model potential*, consistently with the other works. This 316 cm^{-1} figure is also compatible with both the previous MR-AQCC estimate[71] of 301 cm^{-1} and our CC3/aug-cc-pVTZ value of 260 cm^{-1}. Interestingly, determining the CC3 energies on the CCSD or CC2 structures yields similar barrier heights of 269 and 266 cm^{-1}, respectively, indicating that this parameter is not very sensitive to the details of the ES

DOI: 10.1021/acs.jctc.7b00921
J. Chem. Theory Comput. 2017, 13, 6237−6252

Table 4. Geometrical Parameters (Bond Lengths, Å; Valence Angles, Degrees) for the Lowest ES of Ketene, Thioketene, and Diazomethane[a]

	ketene			thioketene			diazomethane		
method	C═O	C═C	C═C═O	C═S	C═C	C═C═S	N═N	C═N	C═N═N
ADC(2)	1.199	1.422	130.6	1.622	1.355	139.7	1.160	1.438	128.6
CC2	1.209	1.428	129.6	1.617	1.365	138.2	1.190	1.408	128.5
CCSD	1.189	1.410	131.8	1.607	1.350	140.7	1.189	1.357	126.7
CCSDR(3)	1.197	1.423	130.0	1.619	1.362	137.4	1.193	1.378	126.1
CC3	1.202	1.427	129.8	1.619	1.367	137.6	1.194	1.385	126.2
CASPT2	1.200	1.425	129.9	1.613	1.367	140.4	1.194	1.382	126.5

[a]All results are obtained with aug-cc-pVTZ and are from the present work. See Tables S5, S6, and S7 in the SI for additional data.

geometry. In contrast, the selected level of theory used to compute the ES energies matters, e.g., the CCSD/def2-TZVPP barrier is 141 cm^{-1} only.

3.3. Thioformaldehyde and Selenoformaldehyde. Thioformaldehyde was much less investigated experimentally than its oxygen counterpart. If an early experimental analysis hinted at a slight puckering in the ES (η of 8.9°),[73] the most recent experimental evidence indicates that H_2C═S remains planar in its lowest ES of A_2 symmetry.[74,75] Consistently, ADC(2), CC2, and CCSD all predict a stable planar minima (absence of imaginary frequencies) for this ES. Selenoformaldehyde is an even more elusive compound and its UV/vis spectroscopic signatures were described only in 1984.[76] For the ES structure, Clouthier and co-workers,[77] concluded that *although information about the out-of-plane mode, ν_4, is incomplete, the correlation with the CH_2S data suggests that CH_2Se is planar or pseudoplanar in [both] excited states.* They confirmed this conclusion in a subsequent work,[78] and again, ADC(2), CC2 and CCSD correctly predict a planar ES minima.

Table 3 lists the geometrical parameters for these two compounds, and a very good match between CASPT2 and CC3 results is again noticeable. As for formaldehyde, a predominantly single-reference wave function is found (0.90 and 0.91 CASPT2 weights for thioformaldehyde and selenoformaldehyde, respectively, T_1 values smaller than 0.2 for both compounds), and we consider the CC3 estimates as the most accurate for these two compounds. For thioformaldehyde, the available experimental estimates of the C═S bond length in the ES,[69,73,74] as well as of the measured elongation of this bond with respect to the GS,[69,74,75] do not allow to set a sufficiently accurate experimental reference value (see Table S3 in the SI), and we have reported the most recent data, 1.682 Å, in Table 3. While the CCSD estimate matches perfectly this value, one clearly notices that the most accurate levels of theory predict significantly longer bonds, that is, 1.709 Å with CC3 and 1.711 Å with CASPT2. In sharp contrast with formaldehyde, CC2 is on the spot for all key ES parameters and this is true for the GS bond lengths and angles as well (see Table S3). ADC(2) overestimates the double-bond length, but to a much lower extent than in formaldehyde (error of ca. + 0.015 Å). Therefore, the previously discussed overestimation of the bond distance by CC2 is not a systematic error even in a homologous series of compounds. This conclusion is confirmed when considering selenoformaldehyde for which the C═Se distance is accurate with CC2, but too long and too contracted with ADC(2) and CCSD, respectively.

3.4. Ketene, Thioketene, and Diazomethane. These three pentatomic compounds present several similitudes. Indeed, in their GS, they belong to the C_{2v} point group, whereas in the (lowest) ES, the C_{2v} structures are unstable (CCSD imaginary frequency of 761$\imath$, 338$\imath$, and 579$\imath$ cm^{-1} for ketene, thioketene, and diazomethane, respectively) and the minima correspond to bent C_s structures, that are rather close to a CI leading back to the GS. Accordingly, these molecules tend to photodissociate quite efficiently and experimental ES structural information are almost nonexistent. Indeed, for ketene, there are, to the best of our knowledge, no experimental data available for ES structures, due to the very rapid photodissociation: no emission spectrum could be recorded. For its thio homologue, there is one experiment by Clouthier, who concluded that the experimental evidence suggest that *the excited-state structure of thioketene is in-plane bent.*[79] For diazomethane, a 1969 work concluded that *the excited state should really be designated A″ in the point group C_s.*[80] On the theoretical side, one can find a very complete CASPT2/6-31+G(d) investigation of the Morokuma group devoted to the dissociation paths of ketene,[81] as well as an earlier investigation of Szalay and co-workers with CC methods for the same molecule.[82] The structure of the lowest ES structure of diazomethane, constrained in the C_{2v} symmetry, was previously determined at both CASPT2/6-31G(d)[26] and CC2/TZVP[25] levels of theory, whereas a CASSCF/6-31G(d) investigation of the ES pathways relating diazirine to diazomethane has also been performed.[83]

The obtained ES parameters are summarized in Table 4. All tested methods agree that the elongations of the C═S and C═C bonds when going from the GS to the ES have rather similar amplitudes in thioketene, but that, in contrast, the terminal bonds (C═O or N═N) extent less than the central ones (C═C or C═N) in ketene and diazomethane. As can be seen in Table S7, ADC(2) and CC2 exaggerate the differences in the latter compound: they predict a too large increase (decrease) of the central (terminal) bond. The data of Table 4 show that CC3 and CASPT2 ES bond lengths are in overall good agreement in most cases, but maybe for the C═S bond of thioketene. The CASPT2 calculations reveal a predominantly single-reference character for all three compounds (dominant configuration weight for the ES: 0.921, 0.869, and 0.900 for ketene, thioketene, and diazomethane, respectively) but the CCSD T_1 diagnostic indicates a significant multiconfigurational character for diazomethane. Therefore, we considered the CC3 values to be the most accurate for the two first compounds, whereas for diazomethane we selected the CASPT2 parameters as benchmark. Interestingly, CCSD systematically gives too short bond lengths and too large valence angles for the parameters listed in Table 4. ADC(2) provides terminal bond lengths on the spot for both ketene (which differs from the C═O in formaldehyde) and thioketene, but significantly too short for diazomethane. For the central bond, the ADC(2) estimate is accurate for ketene, too small for thioketene, and

DOI: 10.1021/acs.jctc.7b00921
J. Chem. Theory Comput. 2017, 13, 6237−6252

Table 5. Comparison between Extrapolated (in Italics) and Actual CC3/aug-cc-pVTZ ES Geometrical Parameters (Rightmost Column; Bond Lengths, Å; Angles, Degrees)[a]

		CCSDR(3)		CC3		
		TZVPP	AVTZ	TZVPP	extrapol	AVTZ
acetylene (A_2)	C≡C	1.3425	1.3402	1.3445	*1.342*	1.342
	C≡C−H	132.03	132.43	132.47	*132.9*	132.9
formaldehyde	C═O	1.3245	1.3203	1.3302	*1.326*	1.326
	η	37.26	36.62	37.38	*36.7*	36.8
thioformaldehyde	C═S	1.7095	1.7052	1.7134	*1.709*	1.709
selenoformaldehyde	C═Se	1.8487	1.8377	1.8538	*1.843*	1.843
ketene	C═O	1.1985	1.1970	1.2031	*1.202*	1.202
	C═C	1.4298	1.4231	1.4344	*1.428*	1.427
	C═C═O	129.64	130.05	129.48	*129.9*	129.8
diazomethane	N═N	1.1968	1.1933	1.1971	*1.194*	1.194
	C═N	1.3822	1.3775	1.3897	*1.385*	1.385
	C═N═N	125.58	126.11	125.72	*126.3*	126.2

[a]The values used for the extrapolation are displayed as well. TZVPP stands for def2-TZVPP and AVTZ for aug-cc-pVTZ. Note that one additional digit has been added to the "raw" values, in order to avoid small deviations due to rounding effects.

Table 6. Geometrical Parameters (Bond Lengths, Å; Valence Angle, Degrees) for the Lowest ES of Nitrosomethane and Nitrosylcyanide[a]

	nitrosomethane			nitrosylcyanide			
method	N═O	C−N	C−N═O	N≡C	C−N	N═O	ref
ADC(2)/aug-cc-pVTZ	1.278	1.460	115.0	1.179	1.306	1.245	this work
CC2/aug-cc-pVTZ	1.270	1.466	117.1	1.207	1.272	1.240	
CCSD/aug-cc-pVTZ	1.222	1.468	119.3	1.162	1.310	1.211	
CCSDR(3)/aug-cc-pVTZ	1.235	1.475	118.4	1.175	1.304	1.223	
CC3/aug-cc-pVTZ	*1.239*	*1.478*	*118.1*	*1.181*	*1.297*	*1.226*	
CASPT2/[b]	1.234	1.479	118.0	1.184	1.304	1.231	
MR-AQCC/cc-pVTZ	1.243	1.486	117.2				88 and 90
experiment				1.198	1.316	1.221	85

[a]The values in italics are basis set extrapolated. [b]CASPT2 with ANO-L-VQZP for nitrosomethane (no frozen core) and aug-cc-pVTZ for nitrosylcyanide. The CASPT2 calculations fail to converge with the diffuse-containing basis set for nitrosomethane.

much too long for diazomethane. For the present set of compounds, the CC2 values are generally reasonable with bond lengths within 0.010 Å of both CC3 and CASPT2 reference values, but for the C═N bond in diazomethane that is significantly too large. The significant deviations of both ADC(2) and CC2 for diazomethane are in line with the result of the T_1 diagnostic test for that molecule.

3.5. First Trends and Structural Basis Set Extrapolation. Though, at this stage, we have considered seven compounds only, a few conclusions already emerged: (i) CC3 and CASPT2 results are in excellent agreement, but such agreement requires the use of a basis set containing diffuse functions for both methods; (ii) CCSDR(3) is a reasonable approximation to CC3, but it typically leads to a small underestimation of the ES double/triple bond lengths by ca. −0.005 Å; (iii) CCSD tends to provide too short multiple bond length by ca. −0.020 Å for the ES; (iv) the errors delivered by both ADC(2) and CC2 seem less systematic, but one notices non-negligible overestimation of the ES bond lengths with the former method in several cases; and (v) for a given molecule, the GS geometry is significantly less sensitive to the method used than its ES counterpart, so that the quality of the former is not a sufficient criterion to ascertain the accuracy of the latter.

As stated in Computational Details, the CC3 calculations imply a huge computational cost, especially when using aug-cc-pVTZ. For this reason, we have used below an extrapolation approach in which the basis set effects obtained at the CCSDR(3) level, that is, the difference between the CCSDR(3)/aug-cc-pVTZ and CCSDR(3)/def2-TZVPP structural parameters, are added to their corresponding CC3/def2-TZVPP values. This procedure is obviously inspired by protocols used previously for transition energies.[84] In Table 5, we provide an illustration of this approach for a series of key parameters that significantly vary with the method being considered. As can be seen, this extrapolation procedure is very effective with no case for which the error is larger than 0.001 Å or 0.1°, justifying its use. In the following as well as in the SI, the values obtained through *basis set extrapolation* are given in italics.

3.6. Nitrosomethane and Nitrosylcyanide. These two compounds contain a nitroso chromogen (N═O), known to yield low-lying ES, and the computed geometries are presented in Tables 6, S8, and S9. For nitrosomethane, experimental evidence points out that it goes from an eclipsed (GS) to a staggered (ES) conformation upon excitation.[85,86] The obtained CCSD results are consistent with the measurements as this method yields an imaginary frequency of 185$\imath$ cm^{-1} (201$\imath$ cm^{-1}) for the staggered (eclipsed) GS (ES) conformer. For the record, the experimentally measured GS rotation barriers are 400 and 383 cm^{-1} (for CD_3NO),[87] whereas we determined a CC3/aug-cc-pVTZ//CCSD/def2-TZVPP value of 428 cm^{-1}. In the ES, measurements indicate an increase of

DOI: 10.1021/acs.jctc.7b00921
J. Chem. Theory Comput. 2017, 13, 6237−6252

the methyl rotation barrier compared to the GS, the most recent estimate for the ES barrier being 475 ± 50 cm^{-1}.[86] Again, the CC3/aug-cc-pVTZ//CCSD/def2-TZVPP value of 507 cm^{-1} is both accurate and very close from a previous MR-AQCC/cc-pVTZ result (522 cm^{-1}).[88] To our knowledge, there is only one experimental investigation available for the ES structure of nitrosylcyanide, N≡C—N═O,[89] and we report, in Table 6, the data considered as the most accurate in that work, though other fits were also performed. For this compound, we attempted to optimize both the trans and cis conformers with CCSD, but the latter led back to the former form.

As for previous molecules, the results listed in Table 6 show the good agreement between the CCSDR(3), CC3, and CASPT2 results with maximal discrepancies of 0.009 Å for the ES bond lengths. Nevertheless, the CCSDR(3) multiple bond lengths seem slightly too short, indicating that the pertubative triple correction is unable to fully rectify the CCSD underestimation. In contrast, the ADC(2) and CC2 N═O bonds are too elongated, especially in nitrosomethane, indicating that the large errors noticed for carbonyl bond distances can also be found in less polarized bonds. For N≡C—N═O, the qualitative impacts of photon absorption predicted by theory, i.e., the significant shortening of the C−N bond and the moderate elongation of the multiple bonds when going from the GS to the ES, are in perfect agreement with the available measurements (see Table S9 in the SI).[89] The absolute ES bond lengths are also reasonably close from their experimental counterparts, though, as expected, such comparison is not sufficient to identify the most accurate level(s) of theory. In both compounds, no significant multireference character is revealed by CASPT2 calculations nor the T_1 diagnostic, and we consider the extrapolated CC3 results as reference values.

3.7. Methylenecyclopropene. The lowest ES of methylenecyclopropene constrained in the C_{2v} point group was studied in detail in ref 28, and we provide a comparison with these previous data in Tables 7 and S10. By comparing our aug-cc-pVTZ CC2 and CASPT2 results to the cc-pVTZ values given in this previous work, we note that the basis set effects are small with CC2, but more significant with CASPT2 for which both C^{ext}═C^{int} and C^{int}═C^{int} bonds become ca. 0.01 Å shorter when diffuse orbitals are added. Overall, the agreement between the different approaches is quite satisfactory, but for the internal double bond. Indeed, for C^{ext}═C^{int} and C^{int}—C^{int}, all methods deliver estimates in the 1.456 ± 0.005 Å and 1.354 ± 0.006 Å ranges, respectively, but CCSD that gives a too contracted C^{ext}═C^{int}. This good agreement holds for the reported valence angle too. In contrast, the ES C^{int}═C^{int} bond is too elongated with both ADC(2) and CC2 but too contracted with CCSD. Our CC3/aug-cc-pVTZ estimate for this bond length is 1.498 Å, 0.015 Å larger than the VMC/pVTZ′ value of 1.483 Å.[28] At this stage it is difficult to determine if this discrepancy is related to the smaller basis set used in the VMC simulations or to the inherent limitations of CC3.

Table 7. Geometrical Parameters (Bond Lengths, Å; Valence Angle, Degrees) for the Lowest ES of Methylenecyclopropene Constrained in the C_{2v} Point Group[a]

method	C^{ext}═C^{int}	C^{int}—C^{int}	C^{int}═C^{int}	C^{ext}═C^{int}—C^{int}	ref
ADC(2)/aug-cc-pVTZ	1.458	1.348	1.515	145.8	this work
CC2/aug-cc-pVTZ	1.454	1.351	1.508	146.1	
CCSD/aug-cc-pVTZ	1.435	1.351	1.476	146.9	
CCSDR(3)/aug-cc-pVTZ	1.450	1.358	1.498	146.5	
CC3/aug-cc-pVTZ	*1.453*	*1.360*	*1.498*	*146.6*	
CASPT2/aug-cc-pVTZ	1.451	1.360	1.488	146.7	
CC2/cc-pVTZ	1.456	1.349	1.512	145.9	28
CASPT2/cc-pVTZ	1.461	1.360	1.496	146.6	
VMC/pVTZ′	1.456	1.351	1.483	146.7	

[a]The values in italics are basis set extrapolated.

3.8. Halogen Derivatives. Numerous tetratomic halogen derivatives of the formaldehyde family have been investigated in the literature with experimental approaches[70,91−103] and, for a few compounds, with high-level theoretical methods as well.[66] We have studied eight compounds in this series, and selected ES parameters are listed in Table 8, whereas complete data can be found in Tables S11−S18 in the SI. For four compounds, the CC3 calculations were beyond reach even with the def2-TZVPP atomic basis set. In all molecules, no significant multireference character was found with CASPT2, and we consequently selected the CC3 (when available) or the CASPT2 (otherwise) data as reference values.

The trends identified for the multiple bonds mirror the conclusions reached for the corresponding non-halogenated compounds: i.e., (i) CCSD delivers too short ES bond lengths; (ii) both ADC(2) and CC2 strongly overestimate the C═O bond lengths (but in F_2C═O) while reasonably estimating C═S and C═Se distances; (iii) CCSDR(3) values are rather accurate but remain slightly too short compared to both CASPT2 and CC3 data, that match well. Interestingly, the puckering angles determined with the three most refined approaches are systematically larger than the values obtained with ADC(2), CC2, and CCSD. In this context, thioformylchloride constitutes a particularly interesting case. To the very best of our knowledge, there is only one experimental work available for ClHC═S and it indicates a weakly twisted ES structure ($\eta \simeq 25°$), with a tiny barrier of 616 cm^{-1} connecting it to the planar ES structure.[97] While CCSD predicts a planar structure (no imaginary frequency in the C_s point group), both ADC(2) and CC2 deliver puckered ES geometries (imaginary frequencies for the planar form) and we have therefore started our CCSDR(3) optimizations using both planar and puckered geometries, and it turned out that the C_1 minimum is the most stable, a conclusion confirmed with CASPT2. For the halogen bonds, the methodological differences across Table 8 are smaller, but CC2 appears to be more accurate for C−F bonds (MAE of 0.002 Å with respect to CASPT2) than for C−Cl bonds (MAE of 0.014 Å). The same observation qualitatively holds for ADC(2), with respective to MAE of 0.007 and 0.030 Å for C−F and C−Cl bonds compared to CASPT2. In contrast the CCSD errors are much more uniform with MAE of 0.007 Å (0.006 Å) for C−F (C−Cl) distances, whereas CCSDR(3) estimates are again accurate (with respect to MAE of 0.003 and 0.002 Å).

An interesting aspect of these structures is the inversion barrier in the ES, for which numerous experimental estimates are available. In the carbonyl series, the experimental barriers rank H_2C═O (316−356 cm^{-1})[68−70,72] < ClHC═O (1609−

DOI: 10.1021/acs.jctc.7b00921
J. Chem. Theory Comput. 2017, 13, 6237−6252

Table 8. Selected ES Geometrical Parameters (Bond Lengths, Å; Angles, Degrees) for Halogen Variants of Formaldehyde, Thioformaldehyde and Selenoformaldehyde[a]

compound	formula	parameter	ADC(2)	CC2	CCSD	CCSDR(3)	CC3	CASPT2	lit.
carbonyldifluoride	$F_2C{=}O$	C=O	1.357	1.367	1.324	1.348	1.353	1.355	1.364[b]
		C−F	1.315	1.324	1.314	1.320	1.323	1.322	1.324[b]
		η	50.5	52.3	54.0	56.1	56.2	52.3	52.6[b], 31.8[b], 30−40[b]
formylfluoride	FHC=O	C=O	1.405	1.394	1.329	1.352	*1.360*	1.360	1.374[b], 1.344[b]
		C−F	1.321	1.334	1.335	1.339	*1.340*	1.335	1.324[b], 1.346[b]
		η	40.4	44.8	45.6	48.3	*48.5*	49.2	43.8[b], 36.0[b]
phosgene	$Cl_2C{=}O$	C=O	1.394	1.365	1.297	1.314		1.319	1.340[b]
		C−Cl	1.701	1.723	1.729	1.738		1.738	1.713[b]
		η	43.3	46.1	48.0	50.3		51.6	44.5[b], 42.0[b]
formyl chloride	ClHC=O	C=O	1.410	1.374	1.304	1.324	*1.331*	1.331	1.356[b], 1.308[b]
		C−Cl	1.687	1.713	1.735	1.742	*1.744*	1.739	1.715[b]
		η	32.9	40.5	41.7	45.2	*45.5*	50.0	39.4[b], 39.4[b]
thiocarbonyldifluoride	$F_2C{=}S$	C=S	1.759	1.765	1.740	1.769	*1.769*	1.770	
		C−F	1.323	1.331	1.319	1.325	*1.328*	1.328	
		θ	38.6	40.4	40.1	43.4	*43.4*	44.9	34.1[b]
thiophosgene	$Cl_2C{=}S$	C=S	1.774	1.755	1.706	1.732		1.736	1.69[b], 1.694[b]
		C−Cl	1.698	1.706	1.707	1.715		1.714	1.756[b], 1.720[b]
		η	27.6	31.0	26.1	32.9		36.1	26.0[b], 23.9[b]
thioformyl chloride	ClHC=S	C=S	1.757	1.737	1.695	1.721		1.725	
		C−Cl	1.699	1.708	1.711	1.717		1.714	
		η	8.9	18.6	0.0	21.9		25.8	25.0[b]
selenocarbonyldifluoride	$F_2C{=}Se$	C=Se	1.884	1.896	1.879	1.910		1.908	
		C−F	1.325	1.331	1.318	1.325		1.328	
		θ	36.7	39.1	39.7	48.7		44.5	30.1[b]

[a]See details in the SI. All results have been obtained with the aug-cc-pVTZ atomic basis set and the values in italics are basis set extrapolated. [b]MR-AQCC/cc-pVTZ results from ref 66. [c]Experimental data from ref 91. [d]Experimental data from ref 70. [e]MR-CISD/cc-pVTZ results from ref 66. [f]Experimental data from ref 92. [g]CASPT2/cc-pVQZ results from ref 66. [h]Experimental data from ref 70. [I]Experimental data from ref 93. [j]Experimental data from ref 94. [k]Experimental data from ref 95. [l]Experimental data from ref 96. [m]Experimental data from ref 97. [n]Experimental data from ref 98.

1642 cm^{-1})[93,103] < FHC=O (2583 cm^{-1})[92] < $Cl_2C{=}O$ (3170−3440 cm^{-1})[70,101] < $F_2C{=}O$ (8200 cm^{-1}).[91] To determine this transition-state barrier, we have used the CC3/aug-cc-pVTZ//CCSD/def2-TZVPP approach. This method delivers exactly the same ordering as experiment: $H_2C{=}O$ (260 cm^{-1}) < ClHC=O (1150 cm^{-1}) < FHC=O (2139 cm^{-1}) < $Cl_2C{=}O$ (2987 cm^{-1} < $F_2C{=}O$ (9495 cm^{-1}). These values are also consistent with previous multireference estimates.[66,71] A similar ordering is found experimentally for the thioformaldehyde derivatives: $Br_2C{=}S$ (465−524 cm^{-1})[104,105] < $Cl_2C{=}S$ (600−620 cm^{-1})[102] < FClC=S (1556 cm^{-1})[106] < $F_2C{=}S$ (3100−3400 cm^{-1}).[94] The corresponding theoretical values are $Br_2C{=}S$ (329 cm^{-1}) < $Cl_2C{=}S$ (375 cm^{-1}) < FClC=S (1541 cm^{-1}) < $F_2C{=}S$ (3786 cm^{-1}). Finally, for $F_2C{=}Se$, the computed barrier (3351 cm^{-1}) exceeds its experimental counterpart (2483 cm^{-1}),[98] as for all difluorine compounds treated here. We compare the theoretical and experimental values in Figure 1, and the reproduction of the trends is obvious, with a linear regression coefficient, R, of 0.99.

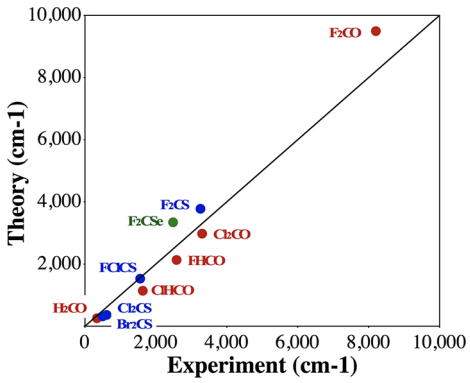

Figure 1. Comparison between theoretical (CC3/aug-cc-pVTZ//CCSD/def2-TZVPP) and experimental ES inversion barriers. Red, blue, and green dots correspond to C=O, C=S, and C=Se derivatives, respectively.

3.9. Statistical Analysis. In this section, we perform a statistical analysis and we report the mean signed (MSE) and absolute (MAE) errors obtained through comparisons with the best theoretical estimates. Though ground-state parameters are not our focus here, we start with the 45 GS bond lengths listed in Tables S1−S18, for which we have systematically taken the CC3/aug-cc-pVTZ result as reference. The results of the statistical analysis are given in Table 9. Globally, all methods provide average errors smaller than 0.010 Å for most GS bond types; that is, they are quite accurate. As it can be seen from the MSE obtained with CC3/def2-TZVPP, the lack of diffuse basis functions yields slightly too long bonds, especially for CN. Both CASPT2 and CC(3) results are extremely close to the CC3 reference, though the bonds are slightly too contracted with these two methods. With CC(3)/def2-TZVPP, there is consequently an error compensation between the basis set and methodological effects, making the final results accurate (MAE of 0.002 Å). For the "lower" methods, one observes an oscillatory behavior: MP2 undershoots the bond lengths on average, CC2 overshoots them, and CCSD underestimates them. The errors are relatively large for the carbonyl bonds

DOI: 10.1021/acs.jctc.7b00921
J. Chem. Theory Comput. 2017, 13, 6237−6252

Table 9. Mean Signed and Absolute Errors (Å) Obtained for Various Methods for the Ground-State (Top) and Excited-State (Bottom) Bond Lengths[a]

	all		CC		CO		CN		CH		CS/CSe			
method	MSE	MAE	MSE	MAE	MSE	MAE	MSE	MAE	MSE	MAE	MSE	MAE	CF/CCl	
						Ground State								
MP2/def2-TZVPP	−0.002	0.005	0.000	0.001	0.001	0.001	0.000	0.009	0.000	0.002	−0.001	0.011	−0.005	0.006
MP2/aug-cc-pVTZ	−0.004	0.005	0.000	0.003	0.001	0.001	0.000	0.011	0.000	0.002	−0.001	0.010	−0.005	0.005
CC2/def2-TZVPP	0.004	0.006	0.004	0.004	0.009	0.009	0.005	0.007	0.000	0.002	0.001	0.004	0.003	0.006
CC2/aug-cc-pVTZ	0.002	0.005	0.001	0.003	0.008	0.008	−0.001	0.011	−0.001	0.001	−0.001	0.002	0.003	0.006
CCSD/def2-TZVPP	−0.005	0.006	−0.004	0.004	−0.007	0.007	−0.002	0.005	0.000	0.001	−0.002	0.009	−0.007	0.008
CCSD/aug-cc-pVTZ	−0.007	0.007	−0.005	0.005	−0.008	0.008	−0.007	0.007	−0.002	0.002	−0.003	0.010	−0.008	0.009
CC(3)/def2-TZVPP	0.001	0.002	0.003	0.003	−0.001	0.001	0.004	0.004	0.002	0.002	0.002	0.002	0.001	0.001
CC(3)/aug-cc-pVTZ	−0.001	0.001	0.000	0.000	−0.002	0.002	−0.002	0.002	0.000	0.000	−0.001	0.001	−0.002	0.002
CC3/def2-TZVPP	0.003	0.003	0.003	0.003	0.001	0.001	0.005	0.005	0.002	0.002	0.003	0.003	0.002	0.003
CASPT2/ANO-L-VQZP	0.001	0.003	0.001	0.002	0.000	0.002	0.004	0.004	0.003	0.003	0.004	0.003	−0.002	0.005
CASPT2/aug-cc-pVTZ	−0.001	0.002	0.000	0.001	−0.002	0.002	−0.001	0.001	0.001	0.002	0.001	0.004	−0.003	0.002
						Excited State								
ADC(2)/def2-TZVPP	0.006	0.016	0.005	0.009	0.043	0.044	0.017	0.024	−0.001	0.002	0.011	0.020	−0.019	0.019
ADC(2)/aug-cc-pVTZ	0.004	0.016	0.000	0.008	0.042	0.043	0.011	0.021	−0.003	0.003	0.011	0.020	−0.020	0.020
CC2/def2-TZVPP	0.006	0.011	0.008	0.010	0.030	0.030	0.009	0.019	0.000	0.002	0.004	0.008	−0.006	0.009
CC2/aug-cc-pVTZ	0.003	0.010	0.003	0.006	0.029	0.029	0.004	0.022	−0.002	0.002	0.002	0.007	−0.007	0.009
CCSD/def2-TZVPP	−0.009	0.010	−0.011	0.011	−0.021	0.021	−0.005	0.016	0.000	0.001	−0.025	0.025	−0.00 6	0.006
CCSD/aug-cc-pVTZ	−0.012	0.013	−0.016	0.016	−0.025	0.025	−0.010	0.017	−0.002	0.002	−0.027	0.027	−0.008	0.008
CCSDR(3)/def2-TZVPP	0.002	0.003	0.003	0.003	−0.002	0.002	0.004	0.006	0.002	0.002	0.005	0.005	0.002	0.004
CCSDR(3)/aug-cc-pVTZ	−0.002	0.003	−0.002	0.003	−0.006	0.006	−0.001	0.005	−0.001	0.001	−0.002	0.003	−0.001	0.002
CC3/def2-TZVPP	0.004	0.004	0.006	0.006	0.003	0.003	0.006	0.006	0.002	0.002	0.006	0.006	0.001	0.001
CASPT2/ANO-L-VQZP	0.002	0.004	0.001	0.003	0.003	0.004	0.003	0.003	0.004	0.004	0.000	0.002	0.003	0.004

[a]The reference values have been obtained at the CC3/aug-cc-pVTZ or CASPT2/aug-cc-pVTZ levels (see text). Note that there is no ANO-L-VQZP basis set defined for selenium, so selenium-bearing molecules were not modeled at the CASPT2/ANO-L-VQZP level.

J. Chem. Theory Comput. 2017, 13, 6237−6252
DOI: 10.1021/acs.jctc.7b00921

with these two latter models. For the present set of compounds, MP2/def2-TZVPP appears as a valuable compromise between accuracy and computational cost with all MAE smaller than or equal to 0.006 Å, but for the CN bonds. From Table 9, it is also clear that the less polarized bonds, i.e., CC and CH, are in general more accurately described than the more polarized ones, i.e., CO, CN, CF, and CCl. Interestingly, CCSD gives almost systematically too short bond distances irrespective of the bond type, whereas the sign of the error is not systematic with MP2 nor CC2.

For the ES, the statistical analysis can be performed for 52 bond lengths and we have selected CC3/aug-cc-pVTZ values as benchmarks, but for the B_u ES of acetylene, diazomethane, and the four compounds of Table 8 for which CC3 calculations were beyond reach, for which we selected CASPT2/aug-cc-pVTZ data as reference. The results are listed in Table 9. The errors tend to be significantly larger than in the ground state, several being above the 0.010 Å threshold. Nevertheless, the global trends noticed for the GS are confirmed. ADC(2) delivers a MAE of 0.016 Å and appears to be especially poor for the carbonyl bond lengths (error > 0.040 Å) and is also insufficiently accurate for CN, CS, and CX bonds. The error pattern is similar in CC2 but with significantly decreased absolute discrepancies compared to ADC(2). For C═O bonds, which are present in many key chromophores of dye chemistry, CC2 overshoots the ES bond length by ca. 0.030 Å, which is not negligible. Resorting to CCSD does not allow one to decrease the absolute errors, but one obtains an almost systematic underestimation of the multiple bond lengths; i.e., one has the advantage of knowing the sign of the error. Only the higher order methods, that is, CCSDR(3) and CASPT2, seem sufficiently accurate to be used as reference values with MAE of ca. 0.003 Å. As in the case of the GS, the lack of diffuse functions in the basis set yields too long bonds, whereas using perturbative triples rather than iterative triples in the CC expansion leads to slightly too compact bonds, with the exception of CN bonds. As a consequence, the CCSDR(3)/def2-TZVPP method emerges as a valuable compromise with no type of bonds presenting an average error larger than 0.005 Å, but CN. Nevertheless, all MSE are positive with this method: the bond distances tend to be slightly too large.

3.10. Additional Molecules. In this section, we briefly discuss additional molecules that have been investigated with (at least) the "best compromise method" determined above, namely, CCSDR(3)/def2-TZVPP. The nature of the minima have been confirmed at the CCSD/def2-TZVPP level. As we have seen for thioformyl chloride, this method might fail in identifying the symmetry of the true minimum for some specific cases but it remains nevertheless the best method that can provide computationally tractable ES vibrational frequencies at this stage. As for the previous systems, detailed data are available in the SI.

Acetaldehyde and Acetone. Like formaldehyde, these molecules undergo puckering in their n → π* ES. For acetaldehyde, we obtain an elongation of the C═O bond of +0.122 Å in the ES, in fair agreement with the only available experiment (+0.11 Å).[107] The computed puckering angle (38.7°) is very similar to the one obtained at the same level of theory in formaldehyde (37.3°). In acetone, this angle significantly increases (42.3°) according to our calculations. For this compound, previous CC2/cc-pVTZ, CASPT2/cc-pVTZ, and VMC/pVTZ' bond lengths are available.[28] The elongation of the carbonyl bond between the GS and the ES obtained with CCSDR(3) (+0.123 Å) is in reasonable agreement with its CASPT2 (+0.136 Å) and VMC (+0.139 Å) counterparts.

Acrolein. Acrolein is a small conjugated molecule that was also included in Guareschi and Filippi's set.[28] The results listed in Table S21 show good agreement between the ES carbonyl bond lengths obtained with CCSDR(3), CASPT2, and VMC theories: 1.324, 1.332, and 1.327 Å, respectively, the CC2 (CCSD) estimate of 1.371 (1.304) Å being too large (too small), consistently with most carbonyl bonds investigated in the present work. For the terminal C═C bond, CCSDR(3) is within 0.006 Å of the VMC estimate (1.377 versus 1.383 Å), but the central ES C−C bond length is most probably too elongated with this method (1.395 Å to be compared to 1.368 Å with VMC and 1.375 Å with CASPT2). Again, the available experimental data[108] do not offer a particularly trustworthy reference to make the final call on the most adequate theory.

Cyanoacetylene. In cyanoacetylene, we optimized two low-lying ES: a bent A″ state (C_s point group) and a Δ state ($C_{\infty v}$ point group). The former induces a strong elongation of the C≡C bond compared to the GS, whereas the latter induces variations more spread throughout the molecule (see Table S22). Previous theoretical works performed with methods lacking dynamic electron correlation,[109,110] provided qualitatively similar results, whereas experimental information is rather limited but confirms the symmetries of the two ES.[111,112]

Cyanoformaldehyde. For this analogue to acrolein, previous ROHF and CASSCF calculations pointed out at a slightly out-of-plane lowest singlet ES,[113,114] with a very flat potential.[113] However, our CCSD calculations deliver a true planar ES minimum (C_s point group). In light of the results obtained for thioformyl chloride, we checked this outcome at both ADC(2) and CC2 levels (Table S23). For the C═O and C≡N bonds, the CCSDR(3) elongations upon excitations are 0.122 and 0.009 Å, respectively. With the same aug-cc-pVTZ basis set, all approaches are rather accurate for the changes of the second bond, whereas for the carbonyl bond elongation, the pattern discussed above is found again, i.e., +0.191, +0.155, and +0.113 Å, with ADC(2), CC2, and CCSD, respectively. In contrast the ES C−C bond length is slight too short/too long with CC2/CCSD (1.375 Å/1.405 Å) compared to CCSDR(3) (1.391 Å).

Cyanogen. For cyanogen, we optimized at the CC3/aug-cc-pVTZ level the lowest excited state of Σ_u^- nature and it turned out to be linear as in the GS, which is consistent with experimental data.[115] We predict a 0.076 Å elongation for the C≡N bond and a −0.081 Å contraction for the C−C bond when going from the GS to the ES. These CC3 changes are close to their CCSDR(3) counterparts and slightly smaller than earlier CASSCF estimates.[109,116]

Diacetylene. In diacetylene, we could locate two different ESs: a bent A_u state in the C_{2h} symmetry and a higher lying Δ_u ES maintaining the cylindrical symmetry of the GS. They both show a more pronounced cumulenic character than the GS, which is consistent with measurements for the latter,[117] experimental information being very thin for the former. The previous theoretical works were, to the best of our knowledge, performed at the Configuration Interaction (CI)[118] and CASSCF[109] levels, and our CCSDR(3) and CC3 estimates of the A_u and Δ_u ESs, respectively, can be viewed as the most accurate available to date.

Glyoxal. For *trans*-glyoxal all measurements foresee elongation and contraction of both the C═O and C−C bonds upon excitation,[108,119,120] and our results are consistent

DOI: 10.1021/acs.jctc.7b00921
J. Chem. Theory Comput. 2017, 13, 6237−6252

with this trend, though the computed variations are about half of their experimental counterparts (see Table S26).

Maleimide. For maleimide, we optimized the lowest B_1 ES, which was considered before at CASSCF[121] and CC2[25] levels of theory, and the results are given in Table S27. The difference between the C−C and C═C bond lengths, which is the bond length alternation, goes from 0.163 Å in the GS to 0.046 Å in the ES according to CCSDR(3), indicating a strong increase of conjugation upon electronic transition. For the ES, the corresponding CASSCF, CC2, and CCSD bond length alternations are 0.035, 0.022, and 0.065 Å, respectively, and the usual bracketing pattern in the CC series is recovered, CC2 (CCSD) providing a too delocalized (localized) description of the ES geometry.

Propenoic Acid Anion. These popular model compounds weres also treated in refs 26 and 28. At the CASPT2 level, the former work predicted strongly different elongations of the two C═O bonds when going to the ES (Table S28), an effect later attributed to an artifact induced by the active space choice,[28] illustrating the challenge of obtaining meaningful CASPT2 results for ES structures. Considering the four bond distances not involving hydrogen atoms, we found MAE of 0.015 and 0.007 Å between our CCSDR(3)/def2-TZVPP values and previous VMC/pVTZ' and CASPT2/cc-pVTZ estimates, respectively,[28] the MAE between the two latter approaches being 0.013 Å.

Pyrazine. For the lowest ES of this heterocylic derivative, we found very small variations of the bond lengths when going from the GS to the ES, the absolute CCSD bond lengths being again too small (Table S29).

(Strepto)cyanine. The shortest model cyanine is known to present a twisted ES,[122] and to avoid this significant relaxation, we have imposed the C_{2v} symmetry in our calculations. Within this constraint, all tested CC levels predict a strong elongation of the CN bond between the GS and the ES, our best estimate being +0.111 Å at the CC3/aug-cc-pVTZ level (Table S30).

Tetrazine. This highly symmetric molecule was studied in detail before,[27,123,124] but not with methods including contributions from triple excitations. As explained in ref 124, one can find a true minimum for the lowest ES of B_{3u} whereas the optimization of the close-lying A_u state leads to a transition-state structure that, after deformation, is found to be on the same adiabatic surface as the B_{3u} ES. Consequently, the states are experimentally mixed and straightforward comparisons between measurements[125−128] and theory are hampered. Both CC3 and CCSDR(3) predict small contractions of all bonds upon excitation and provide results in very good agreement with previous CASPT2 estimates,[123] whereas the CCSD distances seem again too small (Table S31).

Thioacrolein. The lowest ES presents a strongly elongated C═S bond compared to the GS (+0.099 Å). The only experimental data we could find point out at a C_s ES symmetry, with significant elongations of both the C═S and C═C bonds, but no quantitative estimates are provided.[129] As in acrolein, the central C−C ES bond length is too long with CCSD. Together with the underestimation of the ES C═C bond length, this leads to an ES bond length alternation of 0.067 Å with CCSD, almost twice the CCSDR(3) value of 0.035 Å. In other words, CCSD provides a too localized description for the excited state in thioacrolein, as in maleimide.

Thiocarbonyldibromide. For this derivative, the same trends as that for thiophosgene are obtained, CCSD providing shorter C═S and C−X bonds and a smaller puckering angle than CCSDR(3) (see Table S33). The C═S bond length elongation obtained with this latter method (+0.119 Å) fits the available experimental estimate (+0.12 Å).[105]

Thiocarbonylchlorofluoride. For this unsymmetrically substituted thiocarbonyl derivative, we found that the C═S bond length and its extension when going to the ES are both underestimated by CCSD. The same holds for the C−Cl bond and the puckering angle (Table S34).

Trifluoronotrisomethane. According to our calculations, the situation is similar to that of nitrosomethane with an eclipsed GS minimum and a staggered ES minimum. This result is consistent with a previous theoretical investigation,[130] as well as with experimental data,[131] though in an earlier experimental work both staggered and eclipsed conformers could be detected in the ES.[132] We note a fair agreement between our CCSDR(3)/def2-TZVPP bond distances and valence angles and previous MR-AQCC/cc-pVTZ(-f) values;[130] e.g., the ES N═O, C−N, and C−F bond lengths attain 1.233, 1.467, and 1.314 Å at this CC level and 1.245, 1.481, and 1.315 Å with MR-AQCC. As detailed in the SI, the barriers separating the staggered and eclipsed conformations are also well-reproduced by our calculations.

4. CONCLUSIONS

We had two goals when we started this work. On the one hand, we wished to provide a significant database of reliable excited-state geometries to the community, since accurate ES structures, which are hardly accessible through experimental means, were previously described in the theoretical literature only for a very small number of compounds. We have now proposed a database of 35 compounds in which both ground- (35) and excited-states (39) geometrical parameters have been consistently determined with a high-level method including corrections for triple excitations, namely, CCSDR(3)/def2-TZVPP method. These geometries can be viewed as equivalent to those that could be obtained with the GS "golden standard" of quantum chemistry, namely, CCSD(T). This set will therefore allow further calibration and benchmarking work to rely on accurate data to evaluate the accuracy of more computationally effective semiempirical and ab initio methods. On the other hand, we wanted to assess the qualities of the ES geometries determined with "cheap" electron-correlated wave function approaches. To this end, ADC(2), CC2, CCSD, CCSDR(3), CC3, and CASPT2 calculations were systematically carried out for 18 small compounds using extended atomic basis sets. It was gratifying to find that if one correlates all electrons, adds diffuse orbitals in the basis set, and selects a large active space (for CASPT2), one obtains very consistent bond distances and valence angles when choosing either CC3 or CASPT2. Using the CC3/aug-cc-pVTZ results as reference, we have found that all tested methods provide accurate GS data with errors typically smaller than 0.010 Å for all bond types. For the GS, we found that the MP2/def2-TZVPP approach appears as a valuable compromise between accuracy and computational cost for the considered set of molecules. It yields an average error of 0.005 Å, whereas the CCSD/aug-cc-pVTZ method predicts almost systematically too contracted bonds. In the ES, the errors tend to significantly increase compared to the GS, and the dependence on the selected method is also stronger. With ADC(2) and CC2, two very popular second-order models, we obtained a mean absolute deviation on ES bond distances of 0.016 and 0.010 Å, respectively. If these errors are certainly not dramatic, we note that much larger discrepancies

DOI: 10.1021/acs.jctc.7b00921
J. Chem. Theory Comput. 2017, 13, 6237−6252

are found for the CO double-bonds lengths (0.043 and 0.029 Å), which are systematically overshot with these two approaches,. In addition, an average accuracy of 0.010 Å could well be insufficient to reliably benchmark cheaper methods. As in the GS, CCSD provides too compact ES (multiple) distances, which is a trend that is quite consistent for the set of (mainly double and triple) bonds we have considered, but the absolute errors are about twice as large as in the GS (MAE of 0.013 and 0.025 Å for CO bonds). Looking at the bond length alternation in several systems, we found that CCSD tends to provide a too localized description of the ES, whereas CC2 apparently yields the opposite error. Therefore, going from the $O(N^5)$ CC2 to the $O(N^6)$ CCSD approach does not necessarily generate an improvement of the accuracy, though the error trends become more systematic. Eventually, one probably needs to resort to CCSDR(3), or similar methods including contributions from triples, to decrease the average errors to a value of 0.003 Å. This method nevertheless presents the disadvantage of delivering slightly too compact bonds compared to CC3 and CASPT2. As this methodological error presents the opposite sign to the basis set error when a basis set without diffuse functions is chosen, CCSDR(3)/def2-TZVPP indeed appears as a reasonable compromise method to define accurate geometrical parameters for excited-state minima.

■ ASSOCIATED CONTENT

Supporting Information

The Supporting Information is available free of charge on the ACS Publications website at DOI: 10.1021/acs.jctc.7b00921.

List of GS and ES parameters, Cartesian coordinates for selected levels of theory, and description of selected active spaces (PDF)

■ AUTHOR INFORMATION

Corresponding Author

*E-mail: Denis.Jacquemin@univ-nantes.fr.

ORCID

Denis Jacquemin: 0000-0002-4217-0708

Funding

D.J. acknowledges the European Research Council (ERC) and the *Région des Pays de la Loire* for financial support in the framework of a Starting Grant (Marches -278845) and the LumoMat project, respectively. S.B. acknowledges the support of the Scientific Grant Agency VEGA 1/0737/17. This research used resources of (i) the GENCI-CINES/IDRIS, (ii) CCIPL (*Centre de Calcul Intensif des Pays de Loire*), (iii) a local Troy cluster, (iv) HPC resources from ArronaxPlus (Grant ANR-11-EQPX-0004 funded by the French National Agency for Research), and (v) the High Performance Computing Center of the Matej Bel University in Banska Bystrica using the HPC infrastructure acquired in Projects ITMS 26230120002 and 26210120002 (Slovak infrastructure for high performance computing) supported by the Research and Development Operational Programme funded by the ERDF. The collaboration between the French and Slovak teams is supported by Campus France and the Slovak Research and Development Agency through the BridgET Stefanik PHC project.

Notes

The authors declare no competing financial interest.

■ REFERENCES

(1) González, L.; Escudero, D.; Serrano-Andrès, L. Progress and Challenges in the Calculation of Electronic Excited States. *ChemPhysChem* **2012**, *13*, 28−51.

(2) Santoro, F.; Jacquemin, D. Going Beyond the Vertical Approximation with Time-Dependent Density Functional Theory. *WIREs Comput. Mol. Sci.* **2016**, *6*, 460−486.

(3) van Caillie, C.; Amos, R. D. Geometric Derivatives of Excitation Energies Using SCF and DFT. *Chem. Phys. Lett.* **1999**, *308*, 249−255.

(4) Gwaltney, S. R.; Bartlett, R. J. Gradients for the Partitioned Equation-Of-Motion Coupled-Cluster Method. *J. Chem. Phys.* **1999**, *110*, 62−71.

(5) Furche, F.; Ahlrichs, R. Adiabatic Time-Dependent Density Functional Methods for Excited States Properties. *J. Chem. Phys.* **2002**, *117*, 7433−7447.

(6) Köhn, A.; Hättig, C. Analytic Gradients for Excited States in the Coupled-Cluster Model CC2 Employing the Resolution-Of-The-Identity Approximation. *J. Chem. Phys.* **2003**, *119*, 5021−5036.

(7) Scalmani, G.; Frisch, M. J.; Mennucci, B.; Tomasi, J.; Cammi, R.; Barone, V. Geometries and Properties of Excited States in the Gas Phase and in Solution: Theory and Application of a Time-Dependent Density Functional Theory Polarizable Continuum Model. *J. Chem. Phys.* **2006**, *124*, 094107.

(8) Chiba, M.; Tsuneda, T.; Hirao, K. Excited State Geometry Optimizations by Analytical Energy Gradient of Long-Range Corrected Time-Dependent Density Functional Theory. *J. Chem. Phys.* **2006**, *124*, 144106.

(9) Liu, F.; Gan, Z.; Shao, Y.; Hsu, C. P.; Dreuw, A.; Head-Gordon, M.; Miller, B. T.; Brooks, B. R.; Yu, J. G.; Furlani, T. R.; Kong, J. A Parallel Implementation of the Analytic Nuclear Gradient for Time-Dependent Density Functional Theory Within the Tamm−Dancoff Approximation. *Mol. Phys.* **2010**, *108*, 2791−2800.

(10) Gadaczek, I.; Krause, K.; Hintze, K. J.; Bredow, T. Analytical Gradients for the MSINDO-sCIS and MSINDO-UCIS Method: Theory, Implementation, Benchmarks, and Examples. *J. Chem. Theory Comput.* **2012**, *8*, 986−996.

(11) Gyorffy, W.; Shiozaki, T.; Knizia, G.; Werner, H.-J. Analytical Energy Gradients for Second-Order Multireference Perturbation Theory Using Density Fitting. *J. Chem. Phys.* **2013**, *138*, 104104.

(12) Zhang, D.; Peng, D.; Zhang, P.; Yang, W. Analytic Gradients, Geometry Optimization and Excited State Potential Energy Surfaces From the Particle-Particle Random Phase Approximation. *Phys. Chem. Chem. Phys.* **2015**, *17*, 1025−1038.

(13) MacLeod, M. K.; Shiozaki, T. Communication: Automatic Code Generation Enables Nuclear Gradient Computations for Fully Internally Contracted Multireference Theory. *J. Chem. Phys.* **2015**, *142*, 051103.

(14) Vlaisavljevich, B.; Shiozaki, T. Nuclear Energy Gradients for Internally Contracted Complete Active Space Second-Order Perturbation Theory: Multistate Extensions. *J. Chem. Theory Comput.* **2016**, *12*, 3781−3787.

(15) Mendolicchio, M.; Penocchio, E.; Licari, D.; Tasinato, N.; Barone, V. Development and Implementation of Advanced Fitting Methods for the Calculation of Accurate Molecular Structures. *J. Chem. Theory Comput.* **2017**, *13*, 3060−3075.

(16) Dierksen, M.; Grimme, S. The Vibronic Structure of Electronic Absorption Spectra of Large Molecules: A Time-Dependent Density Functional Study on the Influence of *Exact* Hartree-Fock Exchange. *J. Phys. Chem. A* **2004**, *108*, 10225−10237.

(17) Charaf-Eddin, A.; Planchat, A.; Mennucci, B.; Adamo, C.; Jacquemin, D. Choosing a Functional for Computing Absorption and Fluorescence Band Shapes with TD-DFT. *J. Chem. Theory Comput.* **2013**, *9*, 2749−2760.

(18) Muniz-Miranda, F.; Pedone, A.; Battistelli, G.; Montalti, M.; Bloino, J.; Barone, V. Benchmarking TD-DFT against Vibrationally Resolved Absorption Spectra at Room Temperature: 7-Amino-coumarins as Test Cases. *J. Chem. Theory Comput.* **2015**, *11*, 5371−5384.

DOI: 10.1021/acs.jctc.7b00921
J. Chem. Theory Comput. 2017, 13, 6237−6252

(19) Di Tommaso, S.; Bousquet, D.; Moulin, D.; Baltenneck, F.; Riva, P.; David, H.; Fadli, A.; Gomar, J.; Ciofini, I.; Adamo, C. Theoretical Approaches for Predicting the Color of Rigid Dyes in Solution. *J. Comput. Chem.* **2017**, *38*, 998−1004.
(20) Egidi, F.; Williams-Young, D. B.; Baiardi, A.; Bloino, J.; Scalmani, G.; Frisch, M. J.; Li, X.; Barone, V. Effective Inclusion of Mechanical and Electrical Anharmonicity in Excited Electronic States: VPT2-TDDFT Route. *J. Chem. Theory Comput.* **2017**, *13*, 2789−2803.
(21) Guido, C. A.; Jacquemin, D.; Adamo, C.; Mennucci, B. On the TD-DFT Accuracy in Determining Single and Double Bonds in Excited-State Structures of Organic Molecules. *J. Phys. Chem. A* **2010**, *114*, 13402−13410.
(22) Guido, C. A.; Knecht, S.; Kongsted, J.; Mennucci, B. Benchmarking Time-Dependent Density Functional Theory for Excited State Geometries of Organic Molecules in Gas-Phase and in Solution. *J. Chem. Theory Comput.* **2013**, *9*, 2209−2220.
(23) Bousquet, D.; Fukuda, R.; Maitarad, P.; Jacquemin, D.; Ciofini, I.; Adamo, C.; Ehara, M. Excited-State Geometries of Heteroaromatic Compounds: A Comparative TD-DFT and SAC-CI Study. *J. Chem. Theory Comput.* **2013**, *9*, 2368−2379.
(24) Bousquet, D.; Fukuda, R.; Jacquemin, D.; Ciofini, I.; Adamo, C.; Ehara, M. Benchmark Study on the Triplet Excited-State Geometries and Phosphorescence Energies of Heterocyclic Compounds: Comparison Between TD-PBE0 and SAC-CI. *J. Chem. Theory Comput.* **2014**, *10*, 3969−3979.
(25) Tuna, D.; Lu, Y.; Koslowski, A.; Thiel, W. Semiempirical Quantum-Chemical Orthogonalization-Corrected Methods: Benchmarks of Electronically Excited States. *J. Chem. Theory Comput.* **2016**, *12*, 4400−4422.
(26) Page, C. S.; Olivucci, M. Ground and Excited State CASPT2 Geometry Optimizations of Small Organic Molecules. *J. Comput. Chem.* **2003**, *24*, 298−309.
(27) Jagau, T.-C.; Gauss, J. Ground and Excited State Geometries via Mukherjee's Multireference Coupled-Cluster Method. *Chem. Phys.* **2012**, *401*, 73−87.
(28) Guareschi, R.; Filippi, C. Ground- and Excited-State Geometry Optimization of Small Organic Molecules with Quantum Monte Carlo. *J. Chem. Theory Comput.* **2013**, *9*, 5513−5525.
(29) Cleland, D. M.; Per, M. C. Performance of Quantum Monte Carlo for Calculating Molecular Bond Lengths. *J. Chem. Phys.* **2016**, *144*, 124108.
(30) Gozem, S.; Huntress, M.; Schapiro, I.; Lindh, R.; Granovsky, A. A.; Angeli, C.; Olivucci, M. Dynamic Electron Correlation Effects on the Ground State Potential Energy Surface of a Retinal Chromophore Model. *J. Chem. Theory Comput.* **2012**, *8*, 4069−4080.
(31) Gozem, S.; Melaccio, F.; Lindh, R.; Krylov, A. I.; Granovsky, A. A.; Angeli, C.; Olivucci, M. Mapping the Excited State Potential Energy Surface of a Retinal Chromophore Model with Multireference and Equation-of-Motion Coupled-Cluster Methods. *J. Chem. Theory Comput.* **2013**, *9*, 4495−4506.
(32) Huix-Rotllant, M.; Filatov, M.; Gozem, S.; Schapiro, I.; Olivucci, M.; Ferré, N. Assessment of Density Functional Theory for Describing the Correlation Effects on the Ground and Excited State Potential Energy Surfaces of a Retinal Chromophore Model. *J. Chem. Theory Comput.* **2013**, *9*, 3917−3932.
(33) Tuna, D.; Lefrancois, D.; Wolański, Ł.; Gozem, S.; Schapiro, I.; Andruniów, T.; Dreuw, A.; Olivucci, M. Assessment of Approximate Coupled-Cluster and Algebraic-Diagrammatic-Construction Methods for Ground- and Excited-State Reaction Paths and the Conical-Intersection Seam of a Retinal-Chromophore Model. *J. Chem. Theory Comput.* **2015**, *11*, 5758−5781.
(34) Ullrich, C. *Time-Dependent Density-Functional Theory: Concepts and Applications*; Oxford University Press: New York, 2012.
(35) Laurent, A. D.; Jacquemin, D. *Int. J. Quantum Chem.* **2013**, *113*, 2019−2039.
(36) Hellweg, A.; Grün, S. A.; Hättig, C. Benchmarking the Performance of Spin-Component Scaled CC2 in Ground and Electronically Excited States. *Phys. Chem. Chem. Phys.* **2008**, *10*, 4119−4127.
(37) Christiansen, O.; Koch, H.; Jørgensen, P. The Second-Order Approximate Coupled Cluster Singles and Doubles Model CC2. *Chem. Phys. Lett.* **1995**, *243*, 409−418.
(38) Hättig, C.; Weigend, F. CC2 Excitation Energy Calculations on Large Molecules Using the Resolution of the Identity Approximation. *J. Chem. Phys.* **2000**, *113*, 5154−5161.
(39) Hättig, C.; Hald, K. Implementation of RI-CC2 Triplet Excitation Energies With an Application to *Trans*-Azobenzene. *Phys. Chem. Chem. Phys.* **2002**, *4*, 2111−2118.
(40) Dreuw, A.; Wormit, M. The Algebraic Diagrammatic Construction Scheme for the Polarization Propagator for the Calculation of Excited States. *WIREs Comput. Mol. Sci.* **2015**, *5*, 82−95.
(41) Hättig, C. In *Response Theory and Molecular Properties (A Tribute to Jan Linderberg and Poul Jørgensen)*; Jensen, H., Ed.; Advances in Quantum Chemistry; Academic Press: London, 2005; Vol. *50*, pp 37 − 60.
(42) Koch, H.; Jørgensen, P. Coupled Cluster Response Functions. *J. Chem. Phys.* **1990**, *93*, 3333−3344.
(43) Stanton, J. F.; Bartlett, R. J. The Equation of Motion Coupled-Cluster Method - A Systematic Biorthogonal Approach to Molecular Excitation Energies, Transition-Probabilities, and Excited-State Properties. *J. Chem. Phys.* **1993**, *98*, 7029−7039.
(44) Caricato, M. Absorption and Emission Spectra of Solvated Molecules with the EOM−CCSD−PCM Method. *J. Chem. Theory Comput.* **2012**, *8*, 4494−4502.
(45) Caricato, M. Exploring Potential Energy Surfaces of Electronic Excited States in Solution with the EOM-CCSD-PCM Method. *J. Chem. Theory Comput.* **2012**, *8*, 5081−5091.
(46) Christiansen, O.; Koch, H.; Jørgensen, P. Perturbative Triple Excitation Corrections to Coupled Cluster Singles and Doubles Excitation Energies. *J. Chem. Phys.* **1996**, *105*, 1451−1459.
(47) Christiansen, O.; Koch, H.; Jørgensen, P. Response Functions in the CC3 Iterative Triple Excitation Model. *J. Chem. Phys.* **1995**, *103*, 7429−7441.
(48) Andersson, K.; Malmqvist, P. A.; Roos, B. O.; Sadlej, A. J.; Wolinski, K. Second-Order Perturbation Theory With a CASSCF Reference Function. *J. Phys. Chem.* **1990**, *94*, 5483−5488.
(49) Andersson, K.; Malmqvist, P.-A.; Roos, B. O. Second-Order Perturbation Theory With a Complete Active Space Self-Consistent Field Reference Function. *J. Chem. Phys.* **1992**, *96*, 1218−1226.
(50) Granovsky, A. A. Extended Multi-Configuration Quasi-Degenerate Perturbation Theory: The New Approach to Multi-State Multi-Reference Perturbation Theory. *J. Chem. Phys.* **2011**, *134*, 214113.
(51) Frisch, M. J.; Trucks, G. W.; Schlegel, H. B.; Scuseria, G. E.; Robb, M. A.; Cheeseman, J. R.; Scalmani, G.; Barone, V.; Petersson, G. A.; Nakatsuji, H.; Li, X.; Caricato, M.; Marenich, A. V.; Bloino, J.; Janesko, B. G.; Gomperts, R.; Mennucci, B.; Hratchian, H. P.; Ortiz, J. V.; Izmaylov, A. F.; Sonnenberg, J. L.; Williams-Young, D.; Ding, F.; Lipparini, F.; Egidi, F.; Goings, J.; Peng, B.; Petrone, A.; Henderson, T.; Ranasinghe, D.; Zakrzewski, V. G.; Gao, J.; Rega, N.; Zheng, G.; Liang, W.; Hada, M.; Ehara, M.; Toyota, K.; Fukuda, R.; Hasegawa, J.; Ishida, M.; Nakajima, T.; Honda, Y.; Kitao, O.; Nakai, H.; Vreven, T.; Throssell, K.; Montgomery, J. A., Jr.; Peralta, J. E.; Ogliaro, F.; Bearpark, M. J.; Heyd, J. J.; Brothers, E. N.; Kudin, K. N.; Staroverov, V. N.; Keith, T. A.; Kobayashi, R.; Normand, J.; Raghavachari, K.; Rendell, A. P.; Burant, J. C.; Iyengar, S. S.; Tomasi, J.; Cossi, M.; Millam, J. M.; Klene, M.; Adamo, C.; Cammi, R.; Ochterski, J. W.; Martin, R. L.; Morokuma, K.; Farkas, O.; Foresman, J. B.; Fox, D. J. *Gaussian 16*, Revision A.03; Gaussian: Wallingford, CT, USA, 2016.
(52) We stress that applying the frozen-core approximation would affect the results. Indeed, for formaldehyde, thioformaldehyde, and selenoformaldehyde, the use of the frozen-core approximation was found to yield ES C═X bond lengths longer by 0.006, 0.007, and 0.009 Å than their fully correlated counterparts at the EOM-CCSD/aug-cc-pVTZ level. We therefore stick to the full correlation during all CC calculations.

DOI: 10.1021/acs.jctc.7b00921
J. Chem. Theory Comput. 2017, 13, 6237−6252

(53) Lee, T. J.; Taylor, P. R. A Diagnostic for Determining the Quality of Single-Reference Electron Correlation Methods. *Int. J. Quantum Chem.* **1989**, *36*, 199−207.
(54) *TURBOMOLE*, V6.6, a development of University of Karlsruhe and Forschungszentrum Karlsruhe GmbH, 1989−2007; TURBOMOLE: Karlsruhe, Germany, 2014; http://www.turbomole.com (accessed Jun. 13, 2016).
(55) Aidas, K.; Angeli, C.; Bak, K. L.; Bakken, V.; Bast, R.; Boman, L.; Christiansen, O.; Cimiraglia, R.; Coriani, S.; Dahle, P.; Dalskov, E. K.; Ekström, U.; Enevoldsen, T.; Eriksen, J. J.; Ettenhuber, P.; Fernández, B.; Ferrighi, L.; Fliegl, H.; Frediani, L.; Hald, K.; Halkier, A.; Hättig, C.; Heiberg, H.; Helgaker, T.; Hennum, A. C.; Hettema, H.; Hjertenæs, E.; Høst, S.; Høyvik, I.-M.; Iozzi, M. F.; Jansík, B.; Jensen, H. J. A.; Jonsson, D.; Jørgensen, P.; Kauczor, J.; Kirpekar, S.; Kjærgaard, T.; Klopper, W.; Knecht, S.; Kobayashi, R.; Koch, H.; Kongsted, J.; Krapp, A.; Kristensen, K.; Ligabue, A.; Lutnæs, O. B.; Melo, J. I.; Mikkelsen, K. V.; Myhre, R. H.; Neiss, C.; Nielsen, C. B.; Norman, P.; Olsen, J.; Olsen, J. M. H.; Osted, A.; Packer, M. J.; Pawlowski, F.; Pedersen, T. B.; Provasi, P. F.; Reine, S.; Rinkevicius, Z.; Ruden, T. A.; Ruud, K.; Rybkin, V. V.; Sałek, P.; Samson, C. C. M.; de Merás, A. S.; Saue, T.; Sauer, S. P. A.; Schimmelpfennig, B.; Sneskov, K.; Steindal, A. H.; Sylvester-Hvid, K. O.; Taylor, P. R.; Teale, A. M.; Tellgren, E. I.; Tew, D. P.; Thorvaldsen, A. J.; Thøgersen, L.; Vahtras, O.; Watson, M. A.; Wilson, D. J. D.; Ziolkowski, M.; Ågren, H. The Dalton Quantum Chemistry Program System. *WIREs Comput. Mol. Sci.* **2014**, *4*, 269−284.
(56) For the A_u ES of acetylene, the C≡C, C—H, and C≡C—H parameters amount to 1.366 Å (1.368 Å), 1.092 Å (1.090 Å), and 122.4° (122.3°) with cc-pVQZ (aug-cc-pVTZ). For the A_2 ES of the same compound, C≡C, C—H, and C≡C—H attain 1.338 Å (1.340 Å), 1.096 Å (1.093 Å), and 132.3° (132.4°) with cc-pVQZ (aug-cc-pVTZ). For formaldehyde the CCSDR(3)/cc-pVQZ C═O, C—H, H—C—H, and η parameters attain 1.319 Å, 1.089 Å, 118.3°, and 36.7°, respectively. The corresponding CCSDR(3)/aug-cc-pVTZ values are 1.320 Å, 1.089 Å, 118.2°, and 36.6°, respectively.
(57) Vancoillie, S.; Delcey, M. G.; Lindh, R.; Vysotskiy, V.; Malmqvist, P.-Å.; Veryazov, V. Parallelization of a Multiconfigurational Perturbation Theory. *J. Comput. Chem.* **2013**, *34*, 1937−1948.
(58) Aquilante, F.; Autschbach, J.; Carlson, R. K.; Chibotaru, L. F.; Delcey, M. G.; De Vico, L.; Fdez. Galván, I.; Ferré, N.; Frutos, L. M.; Gagliardi, L.; Garavelli, M.; Giussani, A.; Hoyer, C. E.; Li Manni, G.; Lischka, H.; Ma, D.; Malmqvist, P. Å.; Müller, T.; Nenov, A.; Olivucci, M.; Pedersen, T. B.; Peng, D.; Plasser, F.; Pritchard, B.; Reiher, M.; Rivalta, I.; Schapiro, I.; Segarra-Martí, J.; Stenrup, M.; Truhlar, D. G.; Ungur, L.; Valentini, A.; Vancoillie, S.; Veryazov, V.; Vysotskiy, V. P.; Weingart, O.; Zapata, F.; Lindh, R. Molcas 8: New Capabilities for Multiconfigurational Quantum Chemical Calculations across the Periodic Table. *J. Comput. Chem.* **2016**, *37*, 506−541.
(59) Zobel, J. P.; Nogueira, J. J.; Gonzalez, L. The IPEA Dilemma in CASPT2. *Chem. Sci.* **2017**, *8*, 1482−1499.
(60) Aquilante, F.; Pedersen, T. B.; Lindh, R. Low-Cost Evaluation of the Exchange Fock Matrix From Cholesky and Density Fitting Representations of the Electron Repulsion Integrals. *J. Chem. Phys.* **2007**, *126*, 194106.
(61) Huet, T.; Godefroid, M.; Herman, M. The Ã Electronic State of Acetylene: Geometry and Axis-Switching Effects. *J. Mol. Spectrosc.* **1990**, *144*, 32−44.
(62) Herzberg, G. *Molecular Spectra and Molecular Structure. III. Electronic Spectra and Electronic Structure of Polyatomic Molecules*; D. Van Nostrand Company: London, U.K., 1966.
(63) Stanton, J. F.; Gauss, J.; Ishikawa, N.; Head-Gordon, M. A Comparison of Single Reference Methods for Characterizing Stationary Points of Excited State Potential Energy Surfaces. *J. Chem. Phys.* **1995**, *103*, 4160−4174.
(64) Malsch, K.; Rebentisch, R.; Swiderek, P.; Hohlneicher, G. Excited States of Acetylene: A CASPT2 Study. *Theor. Chem. Acc.* **1998**, *100*, 171−182.
(65) Ventura, E.; Dallos, M.; Lischka, H. The Valence-Excited States T_1−T_4 and S_1−S_2 of Acetylene: A High-Level MR-CISD and MR-AQCC Investigation of Stationary Points, Potential Energy Surfaces, and Surface Crossings. *J. Chem. Phys.* **2003**, *118*, 1702−1713.
(66) Bokarev, S. I.; Dolgov, E. K.; Bataev, V. A.; Godunov, I. A. Molecular Parameters of Tetraatomic Carbonyls X_2CO and XYCO (X, Y = H, F, Cl) in the Ground and Lowest Excited Electronic States, Part 1: A Test of Ab Initio Methods. *Int. J. Quantum Chem.* **2009**, *109*, 569−585.
(67) Job, V.; Sethuraman, V.; Innes, K. The 3500 Å $^1A_2$ - X $^1A_1$ Transition of Formaldehyde-h_2, d_2, and hd: Vibrational and Rotational Analyses. *J. Mol. Spectrosc.* **1969**, *30*, 365−426.
(68) Jensen, P.; Bunker, P. The Geometry and the Inversion Potential Function of Formaldehyde in the $\tilde{A}^1$ A_2 and $\tilde{a}^3$ A_2 Electronic States. *J. Mol. Spectrosc.* **1982**, *94*, 114−125.
(69) Clouthier, D. J.; Ramsay, D. A. The Spectroscopy of Formaldehyde and Thioformaldehyde. *Annu. Rev. Phys. Chem.* **1983**, *34*, 31−58.
(70) Godunov, I. A.; Abramenkov, A. V.; Bataev, V. A.; Pupyshev, V. I. Potential Functions of Inversion of R_2CO (R = H, F, Cl) Molecules in the Lowest Excited Electronic States. *Russ. Chem. Bull.* **1999**, *48*, 640−646.
(71) Dallos, M.; Müller, T.; Lischka, H.; Shepard, R. Geometry Optimization of Excited Valence States of Formaldehyde Using Analytical Multireference Configuration Interaction Singles and Doubles and Multireference Averaged Quadratic Coupled-Cluster Gradients, and the Conical Intersection Formed by the $1\,^1B_1(\sigma - \pi^*)$ and $2^1A_1(\pi - \pi^*)$ States. *J. Chem. Phys.* **2001**, *114*, 746−757.
(72) Jones, V.; Coon, J. Rotational Constants and Geometrical Structure of the $^1A_2$ and $^3A_2$ States of H_2CO and D_2CO. *J. Mol. Spectrosc.* **1969**, *31*, 137−154.
(73) Judge, R.; King, G. *J. Mol. Spectrosc.* **1979**, *78*, 51−88.
(74) Jensen, P.; Bunker, P. The Geometry and the Out-Of-Plane Bending Potential Function of Thioformaldehyde in the $\tilde{A}^1A_2$ and $\tilde{a}^3A_2$ Electronic States. *J. Mol. Spectrosc.* **1982**, *95*, 92−100.
(75) Dunlop, J. R.; Karolczak, J.; Clouthier, D. J.; Ross, S. C. Pyrolysis Jet Spectroscopy: The S_1 − S_0 Band System of Thioformaldehyde and the Excited-State Bending Potential. *J. Phys. Chem.* **1991**, *95*, 3045−3062.
(76) Judge, R. H.; Moule, D. C. Detection of a^3A_2(n,)π^* Selenoformaldehyde by Flash Pyrolysis. *J. Am. Chem. Soc.* **1984**, *106*, 5406−5407.
(77) Clouthier, D. J.; Judge, R.; Moule, D. The Laser Excitation Spectrum of Selenoformaldehyde: Vibrational Analyses of the $A^1A_2 \leftarrow X^1A_1$ and $a^3A_2 \leftarrow X^1A_1$ Electronic Transitions. *Chem. Phys.* **1987**, *114*, 417−422.
(78) Clouthier, D. J.; Judge, R.; Moule, D. Selenoformaldehyde: Rotational Analysis of the $\tilde{A}^1A_2$-X $^1A_1$ 735 nm Band System of $H_2C^{78}Se$, $H_2C^{80}Se$, and $D_2C^{78}Se$ from High-Resolution Laser Fluorescence Excitation Spectra. *J. Mol. Spectrosc.* **1990**, *141*, 175−203.
(79) Clouthier, D. J. The Electronic Spectrum of Thioketene and the Excited-State Structure of Ketene. *J. Phys. Chem.* **1987**, *91*, 1354−1357.
(80) Ogilvie, J. F. A. Spectroscopic Study of the Phorodecomposition of Diazomethane. *Photochem. Photobiol.* **1969**, *9*, 65−89.
(81) Xiao, H.; Maeda, S.; Morokuma, K. CASPT2 Study of Photodissociation Pathways of Ketene. *J. Phys. Chem. A* **2013**, *117*, 7001−7008.
(82) Szalay, P. G.; Császár, A. G.; Nemes, L. Electronic States of Ketene. *J. Chem. Phys.* **1996**, *105*, 1034−1045.
(83) Yamamoto, N.; Bernardi, F.; Bottoni, A.; Olivucci, M.; Robb, M. A.; Wilsey, S. Mechanism of Carbene Formation from the Excited States of Diazirine and Diazomethane: An MC-SCF Study. *J. Am. Chem. Soc.* **1994**, *116*, 2064−2074.
(84) Silva-Junior, M. R.; Sauer, S. P. A.; Schreiber, M.; Thiel, W. Basis Set Effects on Coupled Cluster Benchmarks of Electronically Excited States: CC3, CCSDR(3) and CC2. *Mol. Phys.* **2010**, *108*, 453−465.
(85) Ernsting, N. P.; Pfab, J.; Romelt, J. Geometry Changes Accompanying Electronic Excitation of Nitrosomethane in the 650 nm Region. *J. Chem. Soc., Faraday Trans. 2* **1978**, *74*, 2286−2294.

DOI: 10.1021/acs.jctc.7b00921
J. Chem. Theory Comput. 2017, 13, 6237−6252

(86) Gordon, R. D.; Luck, P. Conformational Changes Accompanying Electronic Excitation of CD_3NO. *Chem. Phys. Lett.* **1979**, *65*, 480−483.
(87) Turner, P. H.; Cox, A. P. Microwave Spectrum, Structure, Dipole Moment and Centrifugal Distortion of Nitrosomethane. Dipole Moment of Acetaldehyde. *J. Chem. Soc., Faraday Trans. 2* **1978**, *74*, 533−559.
(88) Dolgov, E. K.; Bataev, V. A.; Pupyshev, V. I.; Godunov, I. A. Ab Initio Description of the Structure and Dynamics of the Nitrosomethane Molecule in the First Excited Singlet and Triplet Electronic States. *Int. J. Quantum Chem.* **2004**, *96*, 589−597.
(89) Dixon, R. N.; Johnson, P. A Rotational Analysis of the $\tilde{A}^1A'' - \tilde{X}^1A'$ Electronic Origin Band of NCNO near 882 nm. *J. Mol. Spectrosc.* **1985**, *114*, 174−184.
(90) Dolgov, E. K.; Bataev, V. A.; Godunov, I. A. Structure of the Nitrosomethane Molecule (CH_3NO) in the Ground Electronic State: Testing of Ab Initio Methods for the Description of Potential Energy Surface. *Int. J. Quantum Chem.* **2004**, *96*, 193−201.
(91) Judge, R. H.; Moule, D. C. Analysis of the 254.7 nm Absorption System of Carbonyl Fluoride. *J. Chem. Phys.* **1983**, *78*, 4806−4810.
(92) Crane, J. C.; Nam, H.; Beal, H. P.; Clauberg, H.; Choi, Y. S.; Moore, C.; Stanton, J. F. Vibrational Assignment of the S_1 Fluorescence Excitation Spectrum of Formyl Fluoride. *J. Mol. Spectrosc.* **1997**, *181*, 56−66.
(93) Ding, H.; Orr-Ewing, A. J.; Dixon, R. N. Rotational Structure in the $\tilde{A}^1A'' - \tilde{X}^1A'$ Spectrum of Formyl Chloride. *Phys. Chem. Chem. Phys.* **1999**, *1*, 4181−4185.
(94) Moule, D.; Mehra, A. The $^1A_2 - {}^1A_1$ Transition in Thiocarbonyl Difluoride at 23477.1 cm^{-1}. *J. Mol. Spectrosc.* **1970**, *35*, 137−148.
(95) Lombardi, J. R. 5142-Å Transition in Thiophosgene ($\pi^* \leftarrow$ n); Rotational Analysis and Excited-State Structure. *J. Chem. Phys.* **1970**, *52*, 6126−6129.
(96) Fujiwara, T.; Lim, E. C.; Kodet, J.; Judge, R. H.; Moule, D. C. The Isotopic Dependence of Axes Switching in Thiophosgene Induced by $A^1A_2(n\pi^*) \leftarrow X^1A_1$ Electronic Excitation. *J. Mol. Spectrosc.* **2005**, *232*, 331−340.
(97) Judge, R. H.; Moule, D. C. Thiocarbonyl Spectroscopy: The $\tilde{A}^1A'' \leftarrow \tilde{X}^1A'$ and $\tilde{a}^3A'' \leftarrow \tilde{X}^1A'$ Electronic Transitions in Thioformyl Chloride, CHCIS. *J. Mol. Spectrosc.* **1985**, *113*, 77−84.
(98) Boluk, M. Y.; Moule, D. C.; Clouthier, D. J. Selenoketone Spectroscopy: Vibronic Analysis of the $\tilde{A}^1A_2 \leftarrow \tilde{X}^1A_1$ and $\tilde{a}^3A_2 \leftarrow \tilde{X}^1A_1$ n → π Electronic Transitions in F_2CSe. *Can. J. Chem.* **1983**, *61*, 1743−1748.
(99) Brand, J. C. D.; Callomon, J. H.; Moule, D. C.; Tyrrell, J.; Goodwin, T. H. The 5340 Å Band System of Thiocarbonyl Chloride. *Trans. Faraday Soc.* **1965**, *61*, 2365−2382.
(100) Fischer, G. The 2670 Å Absorption System of Formyl Fluoride. *J. Mol. Spectrosc.* **1969**, *29*, 37−53.
(101) Moule, D. C.; Foo, P. D. Analysis of the 2973 Å Absorption System of Phosgene. *J. Chem. Phys.* **1971**, *55*, 1262−1268.
(102) Steer, R. P. Structure and Decay Dynamics of Electronic Excited States of Thiocarbonyl Compounds. *Rev. Chem. Intermed.* **1981**, *4*, 1−41.
(103) Judge, R.; Moule, D. The $\tilde{A}^1A'' \leftarrow \tilde{X}^1A'$ Electronic Transition in Formyl Chloride, CHClO. *J. Mol. Spectrosc.* **1985**, *113*, 302−309.
(104) Simard, B.; Hackett, P.; Steer, R. $\tilde{A} - \tilde{X}$ Laser Excitation Spectroscopy of BrClCS and Br_2CS at Room Temperature and in Cold Supersonic Jets. *J. Mol. Spectrosc.* **1987**, *126*, 307−328.
(105) Simard, B.; Steer, R. P.; Judge, R. H.; Moule, D. C. Vibrational Analysis of the Low Resolution $\tilde{a} \leftarrow \tilde{X}$ Absorption Spectra of BrClCS and Br_2CS. *Can. J. Chem.* **1988**, *66*, 359−366.
(106) Subramaniam, C.; Moule, D. Analysis of the $\tilde{A}^1A'' \leftarrow \tilde{X}^1A'$ Electronic Transition in Thiocarbonyl Chlorofluoride. *J. Mol. Spectrosc.* **1974**, *53*, 443−454.
(107) Hubbard, L. M.; Bocian, D. F.; Birge, R. R. The Nature of the $^1n\pi^* \leftarrow S_0$ Transition. 4. The First Excited Singlet State of Acetaldehyde. *J. Am. Chem. Soc.* **1981**, *103*, 3313−3320.
(108) Hollas, J. The electronic Absorption Spectrum of Acrolein Vapour. *SpectroChim. Acta* **1963**, *19*, 1425−1441.
(109) Fischer, G.; Ross, I. G. Electronic Spectrum of Dicyanoacetylene. 1. Calculations of the Geometries and Vibrations of Ground and Excited States of Diacetylene, Cyanoacetylene, Cyanogen, Triacetylene, Cyanodiacetylene, and Dicyanoacetylene. *J. Phys. Chem. A* **2003**, *107*, 10631−10636.
(110) Luo, C.; Du, W. N.; Duan, X. M.; Li, Z. S. A theoretical Study of the Photodissociation Mechanism of Cyanoacetylene in its Lowest Singlet and Triplet Excited States. *Astrophys. J.* **2008**, *687*, 726−730.
(111) Job, V.; King, G. The Electronic Spectrum of Cyanoacetylene: Part I. Analysis of the 2600-Å System. *J. Mol. Spectrosc.* **1966**, *19*, 155−177.
(112) Job, V.; King, G. The Electronic Spectrum of Cyanoacetylene: Part II. Analysis of the 2300-Å System. *J. Mol. Spectrosc.* **1966**, *19*, 178−184.
(113) Clouthier, D. J.; Karolczak, J.; Rae, J.; Chan, W.; Goddard, J. D.; Judge, R. H. Pyrolysis Jet Spectroscopy: The $S_1 - S_0$ Band System of Formyl Cyanide, HCOCN, and DCOCN. *J. Chem. Phys.* **1992**, *97*, 1638−1648.
(114) Ding, W.-J.; Fang, W.-H.; Liu, R.-Z. A Combined CASSCF and TDDFT Study on the Structures and Properties of Formyl Cyanide in Low-Lying Electronic States. *Chem. Phys. Lett.* **2003**, *369*, 570−578.
(115) Fish, G.; Cartwright, G.; Walsh, A.; Warsop, P. Rotational Structure in the $^1\Sigma_u \leftarrow {}^1\Sigma_g^+$ Transition of Cyanogen at 2200 Å. *J. Mol. Spectrosc.* **1972**, *41*, 20−32.
(116) Chaudhuri, R. K.; Krishnamachari, S.; Freed, K. F. Ab Initio Description of the Ground and Excited States of Cyanogen Isomers. *J. Mol. Struct.: THEOCHEM* **2006**, *768*, 119−126.
(117) Bandy, R. E.; Lakshminarayan, C.; Zwier, T. S. Spectroscopy and Photophysics of the $^1\Delta \leftarrow {}^1\Sigma_g^+$ Transition of Jet-Cooled C_4H_2, C_4HD, and C_4D_2. *J. Phys. Chem.* **1992**, *96*, 5337−5343.
(118) Karpfen, A.; Lischka, H. Ab Initio Calculations on the Excited States of π-Systems. II. Valence Excitations in Diacetylene. *Chem. Phys.* **1986**, *102*, 91−102.
(119) Paldus, J.; Ramsay, D. A. The 4 550 Å Band System of Glyoxal I. Rotational Analyses of the (0−0) Bands for $C_2H_2O_2$, C_2HDO_2, and $C_2D_2O_2$. *Can. J. Phys.* **1967**, *45*, 1389−1412.
(120) Birss, F. W.; Braund, D. B.; Cole, A. R. H.; Engleman, R., Jr; Green, A. A.; Japar, S. M.; Nanes, R.; Orr, B. J.; Ramsay, D. A.; Szyszka, J. The 4 550 Å Band System of Glyoxal. IV. Vibration−Rotational Analyses for 11 Bands of $^{13}C_2H_2O_2$ and Determination of Molecular Geometries. *Can. J. Phys.* **1977**, *55*, 390−395.
(121) Climent, T.; González-Luque, R.; Merchán, M. Theoretical Analysis of the Excited States in Maleimide. *J. Phys. Chem. A* **2003**, *107*, 6995−7003.
(122) Send, R.; Valsson, O.; Filippi, C. Electronic Excitations of Simple Cyanine Dyes: Reconciling Density Functional and Wave Function Methods. *J. Chem. Theory Comput.* **2011**, *7*, 444−455.
(123) Schütz, M.; Hutter, J.; Lüthi, H. P. The Molecular and Electronic Structure of s-Tetrazine in the Ground and First Excited State: A Theoretical Investigation. *J. Chem. Phys.* **1995**, *103*, 7048−7057.
(124) Stanton, J. F.; Gauss, J. The First Excited Singlet State of s-Tetrazine: A Theoretical Analysis of Some Outstanding Questions. *J. Chem. Phys.* **1996**, *104*, 9859−9869.
(125) Meyling, J. H.; Van Der Werf, R. P.; Wiersma, D. A. Excited State Geometry of and Radiationless Processes in the Lowest $B_{3u}(n\pi^*)$ Singlet State of s-Tetrazine. *Chem. Phys. Lett.* **1974**, *28*, 364−372.
(126) Smalley, R. E.; Wharton, L.; Levy, D. H.; Chandler, D. W. The Fluorescence Excitation Spectrum of s-Tetrazine Cooled in a Supersonic Free Jet. *J. Mol. Spectrosc.* **1977**, *66*, 375−388.
(127) Job, V. A.; Innes, K. K. The Geometric Structure of s-Tetrazine and Its Change on Electronic Excitation. *J. Mol. Spectrosc.* **1978**, *71*, 299−311.
(128) Innes, K. K.; Brumbaugh, D. V.; Franks, L. A. Franck-Condon Analysis of Visible Absorption of s-Tetrazine Vapor. *Chem. Phys.* **1981**, *59*, 439−442.
(129) Judge, R. H.; Moule, D. C. A Vibronic Analysis of the Lower $\tilde{A}^1A'' \leftarrow \tilde{X}^1A'$ Singlet−Singlet and $\tilde{a}^3A'' \leftarrow \tilde{X}^1A'$ Triplet−Singlet Band

DOI: 10.1021/acs.jctc.7b00921
J. Chem. Theory Comput. 2017, 13, 6237−6252

Systems of Thioacrolein (2-Propenethial). *J. Chem. Phys.* **1984**, *80*, 4646−4650.
(130) Dolgov, E. K.; Bataev, V. A.; Pupyshev, V. I.; Godunov, I. A. Structure and Vibrations of the CF_3NO Molecule in the Ground and Lowest Excited Electronic States: A Test of Ab Initio Methods. *Int. J. Quantum Chem.* **2004**, *100*, 509−518.
(131) Dyet, J.; McCoustra, M.; Pfab, J. The Visible Spectrum of Jet-Cooled CF_3NO. *Chem. Phys. Lett.* **1987**, *135*, 534−538.
(132) Gordon, R. D.; Dass, S. C.; Robins, J. R.; Shurvell, H. F.; Whitlock, R. F. Conformational Changes Accompanying Electronic Excitation of Trifluoronitrosomethane. *Can. J. Chem.* **1976**, *54*, 2658−2668.

DOI: 10.1021/acs.jctc.7b00921
J. Chem. Theory Comput. 2017, 13, 6237−6252